

**PURDUE UNIVERSITY  
GRADUATE SCHOOL  
Thesis/Dissertation Acceptance**

This is to certify that the thesis/dissertation prepared

By Vaibhav V Gokhale

Entitled

DESIGN OF A HELMET WITH AN ADVANCED LAYERED COMPOSITE FOR ENERGY DISSIPATION USING A MULTI-MATERIAL COMPLIANT MECHANISM SYNTHESIS

For the degree of Master of Science in Mechanical Engineering

Is approved by the final examining committee:

Andres Tovar

Chair

Khosrow Nematollahi

Likun Zhu

To the best of my knowledge and as understood by the student in the Thesis/Dissertation Agreement, Publication Delay, and Certification Disclaimer (Graduate School Form 32), this thesis/dissertation adheres to the provisions of Purdue University's "Policy of Integrity in Research" and the use of copyright material.

Approved by Major Professor(s): Andres Tovar

Approved by: Jie Chen

Head of the Departmental Graduate Program

7/5/2016

Date

DESIGN OF A HELMET WITH AN ADVANCED LAYERED COMPOSITE FOR  
ENERGY DISSIPATION USING A MULTI-MATERIAL COMPLIANT  
MECHANISM SYNTHESIS

A Thesis

Submitted to the Faculty

of

Purdue University

by

Vaibhav V Gokhale

In Partial Fulfillment of the

Requirements for the Degree

of

Master of Science in Mechanical Engineering

August 2016

Purdue University

Indianapolis, Indiana

Dedicated to my mother

## ACKNOWLEDGMENTS

I would like to convey my gratitude to all people who supported me in this venture. My adviser Dr. Andrés Tovar constantly helped me right from the beginning of the Masters course. He gave me a fantastic idea for research and constantly motivated to produce good results. His guidance proved invaluable not only for the research, but also for my overall personal and professional progress.

Mr. Darin Grice, president of Turtle shell protective systems, Indianapolis worked with our group for a project similar to this thesis. Experience of that work was advantageous for me during this research. My thesis committee members Dr. Khosrow Nematollahi and Dr. Likun Zhu provided me with many precious inputs which were helpful in enhancing quality of my work. I am thankful to all of my friends for being with me throughout this journey. My special thanks to labmates from SL041 lab: Prathamesh Chaudhari, Prasad Mehta, Sajjad Raeisi, Ehsan Malekipour, Samuel Attoye, Deepak Kumar Tangirala and Anurag Deb.

Lastly, a big hearty thanks to my parents and all family members because of whom I could pursue advanced education and could surpass all the hardships.

## TABLE OF CONTENTS

	Page
LIST OF TABLES . . . . .	vii
LIST OF FIGURES . . . . .	viii
ABBREVIATIONS . . . . .	x
ABSTRACT . . . . .	xi
1 INTRODUCTION . . . . .	1
1.1 Traumatic Brain Injuries (TBI) . . . . .	1
1.1.1 Statistics about TBI . . . . .	1
1.1.2 Biomechanics of TBI . . . . .	3
1.2 Impact Protective Structures . . . . .	5
1.2.1 Objectives of Impact Protective Structures . . . . .	5
1.2.2 Different Types of Helmet Designs . . . . .	6
1.2.3 Components of a Sports Helmet . . . . .	7
1.2.4 Measurement of Helmet Performance . . . . .	9
1.3 Shortcomings of the Existing Designs . . . . .	9
1.4 Recent Developments and Non Traditional Energy Absorbing Structures Used in Modern Helmets . . . . .	10
1.5 Proposed Solution . . . . .	13
1.5.1 Outer Hard Shell . . . . .	15
1.5.2 Compliant Buffer Zone (CBZ) . . . . .	15
1.5.3 Inner Layer . . . . .	15
2 DESIGN PROCEDURE . . . . .	16
2.1 Design of Compliant Mechanism . . . . .	16
2.1.1 Topology Optimization . . . . .	17
2.2 Conceptual 2D Design of Compliant Mechanism . . . . .	18

	Page
2.2.1 Numerical Formulation . . . . .	18
2.2.2 Problems Due to Thin Hinges . . . . .	21
2.2.3 Multi-Material Topology Optimization of the Compliant Mechanism . . . . .	22
2.3 3D Compliant Mechanism . . . . .	24
2.4 Design of Connections Among Compliant Mechanisms . . . . .	24
2.5 Design of Complete ALC . . . . .	27
2.6 Conceptual Design of Helmet Using ALC . . . . .	28
2.6.1 Inner Comfort Foam . . . . .	28
2.6.2 ALC Within the Helmet Material System . . . . .	29
2.6.3 Front Protective Shield . . . . .	29
2.7 Polyjet Additive Manufacturing Technique . . . . .	31
2.8 Selection of Materials for Different Components of ALC . . . . .	33
2.8.1 Materials for the Top Hard Shell . . . . .	33
2.8.2 Materials for the CBZ . . . . .	34
2.8.3 Material for the Inner Core . . . . .	36
3 PERFORMANCE ASSESMENT OF ALC UNDER IMPACT LOAD . . . . .	37
3.1 Test Setup . . . . .	37
3.2 Results for Linear Impact . . . . .	41
3.2.1 Kinetic Energy . . . . .	41
3.2.2 Linear Force . . . . .	43
3.2.3 Max von Mises Stress on the Outer Hard Shell . . . . .	44
3.2.4 Maximum Strain on the Outer Shell . . . . .	45
3.3 Oblique Impact . . . . .	45
3.3.1 Kinetic Energy . . . . .	46
3.3.2 Linear Force . . . . .	46
3.3.3 Max von Mises Stress on the Outer Shell . . . . .	47
3.3.4 Maximum Strain on the Outer Shell . . . . .	48

	Page
4 SUMMARY AND CONCLUSION . . . . .	51
4.1 Summary . . . . .	51
4.2 Conclusion . . . . .	51
4.3 Original Contribution . . . . .	52
4.4 Future Work . . . . .	53
LIST OF REFERENCES . . . . .	55

## LIST OF TABLES

Table	Page
1.1 Statistics about head concussion in NFL (source: Frontline U.S. TV series). . . . .	3
2.1 Mechanical properties of polycarbonate. . . . .	34
2.2 Mechanical properties of ABS. . . . .	35
2.3 Mechanical properties of TangoBlackPlus. . . . .	35
3.1 Table about information of various element types used. . . . .	38
3.2 Table of material density, elastic modulus and material models. . . . .	39
3.3 Time of contact for linear impact. . . . .	42
3.4 Peak linear force for linear impact . . . . .	44
3.5 Max strain (%) for subcases of linear impact. . . . .	45
3.6 Time of contact for oblique impact. . . . .	47
3.7 Peak linear force for oblique impact. . . . .	48
3.8 Max strain (%) for subcases of oblique impact. . . . .	50



## LIST OF FIGURES

Figure	Page
1.1 Causes of TBI Source: United States Centers for Disease Control and Prevention (CDC). . . . .	2
1.2 Swelling of brain at the exterior parts in coup-countercoup injuries (Source: <a href="http://spiutica.com/blog-article-concussion-in-sports/">http://spiutica.com/blog-article-concussion-in-sports/</a> ). . . . .	3
1.3 Breaking of axons due to large shearing forces (Source: <a href="http://www.tbibraininjurysurvivor.com">www.tbibraininjurysurvivor.com</a> ). . . . .	4
1.4 Cross section of a helmet with names of different components. . . . .	7
1.5 Section of a Schutt DNA helmet showing TPU cushioning and other parts (Source: <a href="https://www.schuttsports.com/science-of-domination">https://www.schuttsports.com/science-of-domination</a> ). . . . .	10
1.6 Zenith helmet with air cushioning for energy absorption (Source: <a href="http://www.xenith.com/pages/xenith-technology">http://www.xenith.com/pages/xenith-technology</a> ). . . . .	11
1.7 A 6d helmet with omni directional suspension system implemented together with EPS foam (Source: <a href="http://www.6dhelmets.com/innovation/">http://www.6dhelmets.com/innovation/</a> ). . . . .	12
1.8 Smith optics Koroyd straws helmet (Source: <a href="http://www.smithoptics.com/us/techhelmet">http://www.smithoptics.com/us/techhelmet</a> ). . . . .	13
1.9 D30 trust helmet pad system (Source: <a href="http://www.d3o.com/">http://www.d3o.com/</a> ). . . . .	14
1.10 Concept of the proposed solution. . . . .	14
2.1 Classic force inverter compliant mechanism ( <i>C.H. Liu, G.F. Huang, "A Topology Optimization Method With Constant Volume Fraction During Iterations for Design of Compliant Mechanisms", J. Mechanisms Robotics, vol.8, no. 4, 2015</i> ). . . . .	18
2.2 Initial design domain, loads and boundary conditions used for 2D topology optimization of compliant mechanism. . . . .	19
2.3 Result of single material topology optimization. . . . .	20
2.4 3D printed compliant mechanism with only one material. . . . .	21
2.5 Finite element analysis showing failure due to stress concentration. . . . .	22

Figure	Page
2.6 Result of multi-material topology optimization of the compliant mechanism. . . . .	23
2.7 3D axis symmetric compliant mechanism. . . . .	25
2.8 Input displacement vs output displacement of 3D compliant mechanism.	25
2.9 Force vs displacement graph for 3D compliant mechanism. . . . .	26
2.10 Flexible rubber spring for connecting compliant mechanisms. . . . .	27
2.11 Graph of force vs. displacement for the rubber spring. . . . .	28
2.12 Complete design of ALC. . . . .	29
2.13 The innermost comfort foam with slots for the threaded holes. . . . .	30
2.14 The CAD model of integrated ALC with representation of different regions. . . . .	30
2.15 Conceptual design of a helmet using ALC. . . . .	31
2.16 Working of a polyjet 3D printer ( <a href="http://3dprinterblog.net/polyjet-3d-printing/">http://3dprinterblog.net/polyjet-3d-printing/</a> ). . . . .	32
3.1 Description of the test setup . . . . .	38
3.2 Subcases of linear impact. . . . .	40
3.3 Subcases of oblique impact . . . . .	41
3.4 Kinetic energy for subcases of linear impact. . . . .	42
3.5 Linear force for subcases of linear impact. . . . .	43
3.6 Contours and maximum values of von Mises stresses on the outer hard shell for subcases of linear impact. . . . .	44
3.7 Kinetic energy for oblique impact at 30°. . . . .	46
3.8 Kinetic energy for oblique impact at 60°. . . . .	47
3.9 Linear force for oblique impact at 30°. . . . .	48
3.10 Linear force for oblique impact at 60°. . . . .	49
3.11 Contours and maximum values of von Mises stresses on the outer hard shell for subcases of oblique impact. . . . .	49

## ABBREVIATIONS

2D	Two Dimensional
3D	Three Dimensional
ABS	Acrylonitrile Butadiene Styrene
ALC	Advanced Layered Composite
ATDs	Anthropomorphic Test Devices
CAD	Computer Aided Design
CBZ	Compliant Buffer Zone
CT	Computed Tomography
DAI	Diffuse Axonal Injury
EPP	Expanded Polypropylene
EPS	Expanded Polystyrene
GCS	Glasgow Trauma Scale
HIC	Head Injury Criterion
NBR	Nitrile Butadiene Rubber
NFL	National Football League
NVH	Noise, Vibration and Harshness
PC	Polycarbonate
PRBM	Pseudo Rigid Body Model
SIMP	Solid Isotropic Material with Penalization
TBI	Traumatic Brain Injuries
TPU	Thermoplastic Polyurethane

## ABSTRACT

Gokhale, Vaibhav V. M.S.M.E., Purdue University, August 2016. Design of a Helmet With an Advanced Layered Composite for Energy Dissipation Using a Multi-material Compliant Mechanism Synthesis. Major Professor: Andrés Tovar.

Traumatic Brain Injuries (TBI) are one of the most apprehensive issues today. In recent years a lot of research has been done for reducing the risk of TBI, but no concrete solution exists yet. Helmets are one of the protective devices that are used to prevent human beings from mild TBI. For many years some kind of foam has been used in helmets for energy absorption. But, in recent years non-traditional solutions other than foam are being explored by different groups. Focus of this thesis is to develop a completely new concept of energy absorption for helmet liner by diverting the impact forces in radial directions normal to the direction of impact.

This work presents a new design of an advanced layered composite (ALC) for energy dissipation through action of a 3D array of compliant mechanisms. The ALC works by diverting incoming forces in multiple radial directions and also has design provisions for reducing rotational forces. Design of compliant mechanism is optimized using multi-material topology optimization algorithm considering rigid and flexible material phases together with void. The design proposed here needs to be manufactured using the advanced polyjet printing additive manufacturing process. A general and parametric design procedure is explained which can be used to produce variants of the designs for different impact conditions and different applications.

Performance of the designed ALC is examined through a benchmark example in which a comparison is made between the ALC and the traditional liner foam. An impact test is carried out in this benchmark example using dynamic Finite Element Analysis in LS DYNA. The comparison parameters under consideration are gradu-

alness of energy absorption and peak linear force transmitted from the ALC to the body in contact with it. The design in this article is done particularly for the use in sports helmets. However, the ALC may find applications in other energy absorbing structures such as vehicle crashworthy components and protective gears. The ultimate goal of this research is to provide a novel design of energy absorbing structure which reduces the risk of head injury when the helmet is worn.

## 1. INTRODUCTION

### 1.1 Traumatic Brain Injuries (TBI)

Traumatic brain injuries (TBI) have been a serious issue for decades. TBI are a form of acquired brain injury caused when head suddenly and violently hits an object. In severe TBI the object pierces the skull and enters brain tissues. These types of injuries are substantially reduced in recent years due to increased strength of the outer shells of the helmets. However, most of the TBI occur even when there is no direct piercing of the object into the skull. Such injuries are called mild Traumatic Brain Injuries (mTBI). Mild traumatic brain injuries are also known as concussions.

A cranial Computed Tomography (CT) scan is a standard test to assess the brain after injury. Severity of TBI differs in each case and is assessed based on Glasgow Coma Scale (GCS) [1]. TBI causes many consequences like headache, nausea, vomiting, dizziness, fatigue, sleep disturbance, etc. as well as long term effects like Alzheimers disease, major depression, memory loss, etc [2]

#### 1.1.1 Statistics about TBI

According to the statistics released by the United States Center for Disease Control and Prevention (CDC), every day 138 people from U.S. die of TBI. These are causes behind 30% of the total deaths. In 2010, 2.5 million Emergency Department (ED) visits, 280,000 hospitalizations, 50,000 deaths were reported.

Figure 1.1 shows causes of TBI with the corresponding share in total TBI cases for the years 2006-2010. Major causes include road accidents, struck by or against, falls (mainly caused in old people and children), assaults and some other unidentified causes. Falls are the most frequent causes of TBI. Struck by or against have the second

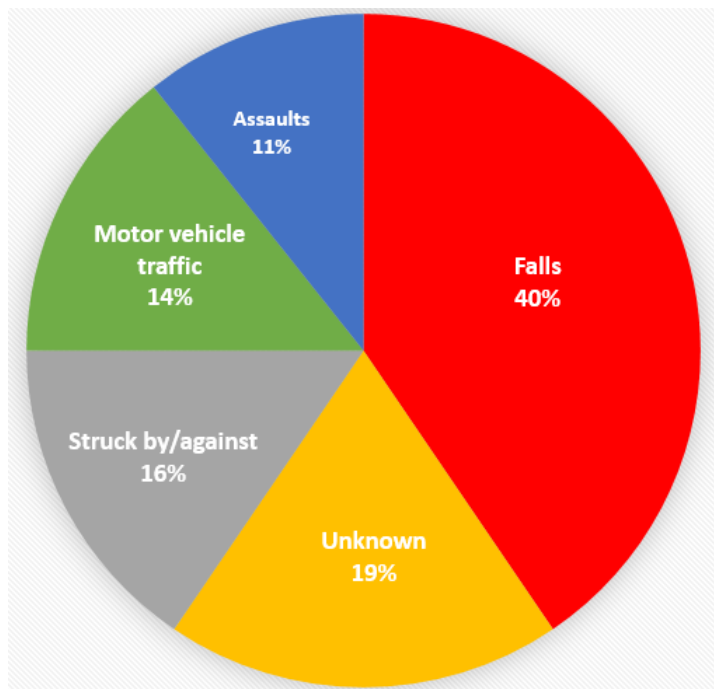


Fig. 1.1. Causes of TBI Source: United States Centers for Disease Control and Prevention (CDC).

highest share. These include very infamous sports concussions which come under the category of blunt trauma [2]. Sports in which there is a high risk of concussions are: ice hockey, American football, soccer, wrestling and lacrosse. Cases of TBI found in girls sports are more than those found in boys sports.

Statistics about the reported head concussions in NFL are as given in Table 1.1. These are the statistics only recorded during NFL league games. TBI those occur during practice and in collegiate football players are large in numbers and those are not included in these statistics. Motor vehicle traffic has the third highest share. To alleviate the damage in car accidents various crash avoidance and crashworthiness measures are implemented.

Total 22,594 numbers of service members were diagnosed with mild TBI in 2015 as reported by Defense and Veterans Brain Injury Center (DVBIC) during day to day activities such as recreational sports, military deployment and training. All these

Table 1.1  
 Statistics about head concussion in NFL (source: Frontline U.S. TV series).

Year	Number of concussions
2012	171
2013	152
2014	123
2015	199

statistics convey severity of TBI and importance of finding more and more impact attenuating solutions for the safety of human beings.

### 1.1.2 Biomechanics of TBI

TBI are not completely revealed. These are topics of ongoing research for medical field. Various forces like linear forces, rotational forces and angular forces or a combination of these forces are responsible for TBI. Two main types of TBI can be identified from the research that has been done till the date. These are: Coup Countercoup injuries and Diffuse Axonal Injuries (DAI) [1].

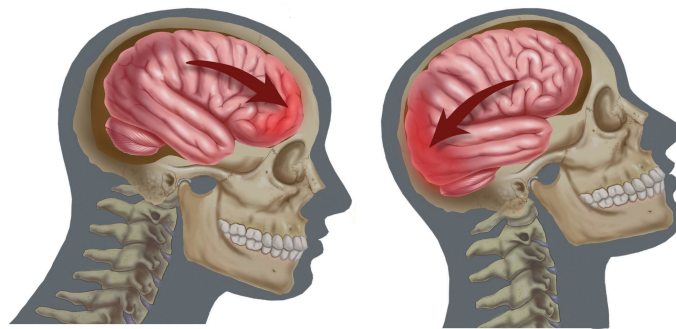


Fig. 1.2. Swelling of brain at the exterior parts in coup-counter coup injuries  
 (Source: <http://spiutica.com/blog-article-concussion-in-sports/>).



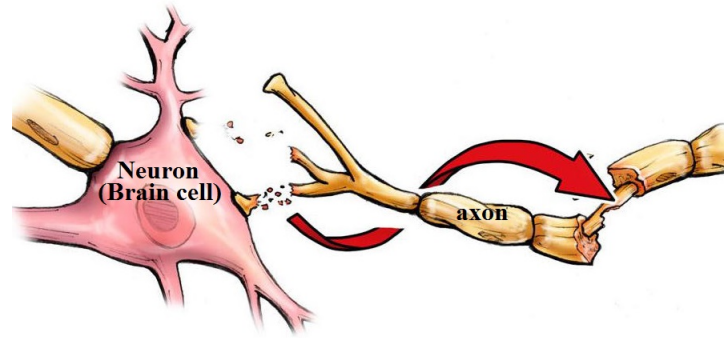


Fig. 1.3. Breaking of axons due to large shearing forces  
(Source: [www.tbibraininjurysurvivor.com](http://www.tbibraininjurysurvivor.com)).

Brain is one of the most fragile organs in the human body. It is encased in the skull and surrounded by a gelatinous layer of fluid known as cerebrospinal fluid. This layer provides a cushioning to the brain. When a moving head is suddenly stopped, brain breaks the gelatinous fluid layer due to its moment of inertia and bounces against the bony interior of the skull. This causes swelling of the brain on the outer surface. This type of injury is called coup-countercoup injury [1]. In low speed coup-countercoup injury, damage caused to the brain may not be visible to the naked eye. When the impact velocity is high, the damage caused to the brain is also very high.

There are over 100 billion nerve cells called neurons. Neurons have main cell body and extensions called dendrites. Axons connect multiple neurons. Axons are important for communication among different brain parts. Axons are extremely thin and fragile. When brain moves, parts of the brain having different densities move with different velocities. Axons crossing these junctions are subjected to high shearing forces. In Diffuse Axonal Injury (DAI), axons break in such situations. When axons are broken, neurons lose network among them and they are unable to transmit signals. Over the period, brain cells become dead. Functions of brain associated with the corresponding cells are affected [1].

## 1.2 Impact Protective Structures

Skull does not absorb the impact energy. It is a poor shock absorber. Hence, in order to prevent head injuries some energy absorbing structures must be implemented. Vehicle bodies have crashworthy components which are made up of thin metal tubes that absorb the energy through buckling and progressive collapse in the form of strain energy. Some components made up of aluminum foam are also placed in the frame assembly for energy absorption. Helmets are used to protect head for preventing head injuries in sports, combats as well as cars and bikes races. High density viscoelastic foams are used in helmets. For this thesis, our focus is on helmets. However, the invention to be presented in the following chapters is intended to be used in all impact protective structures like car crashworthy components and protective gears.

### 1.2.1 Objectives of Impact Protective Structures

Before the discovery of TBI, the job of the helmets was to just protect the skull from the direct damage. The ultimate objective was to prevent the intrusion of the object. Those helmets were made up of only a metal layer or of leather. Then, plastic helmets with foams as energy absorbing elements were introduced. These kinds of helmets are still in use. The designs of these helmets are based on the criterion of absorbing maximum energy. As the research is progressing greatly about the mechanisms of TBI, another requirement of the helmet design is being enlightened which is gradual absorption of impact energy. Hence, objectives for a good design of an impact protective structure should be as follows [3].

- Prevent intrusion of the object
- Absorb maximum energy per unit volume (specific energy absorption)
- Produce a deceleration pulse with early peak and gradual decay

### 1.2.2 Different Types of Helmet Designs

- Construction helmets

Construction helmets designed for lesser impacts do not necessarily have foam inside. Most of the helmets are just hard plastic shells. A few are hard shells with suspension bands to obtain a fit and keep space for the circulation of the air. These helmets are designed for very minimal energy absorption. These helmets are intended to protect the head from the fall of construction materials like bricks. Similar helmets are sometimes used as safety helmets in mechanical manufacturing facilities and other work sites where safety is required.

- Bicycle helmets

Bicycle helmets have a crushable foam inside them. They are not designed for repeated impacts. If bicycle helmet undergoes an impact, the foam is trashed and it cannot be used again. These helmets are also not designed to sustain very high velocity or in other words very severe impacts. The thickness of the outer shell is very less and consequently its impact strength is also less. The foam used for these helmets is usually low-medium density Expanded Polystyrene foam [4].

- Sports helmets

If the helmet is made for hockey, football or skateboarding, then behavior of the foam must be squishy and should have a slow rebound. The foams used for energy absorption are non-crushable foams. The outer hard shell has more thickness and consequently high impact strength.

Some of the foam materials that are used in these types of helmets are: Butyl Nitrate or Expanded Polypropylene or Vinyl-Nitrile foam [5]. Motorcycle helmets or racing helmets have similar construction and dimensions. However, these are made up of a crushable foam [6]. Cost of these helmets is high compared to the bike helmets.

- Ballistic helmets

Ballistic helmets are different and they use various composites. (Accordingly the testing criteria also differ, i.e. ballistic helmets have to pass the most severe testing and bicycle helmets have to pass the least severe testing). The outer shell of ballistic helmets is extremely strong as compared to the other helmets. These helmets are supposed to prevent injuries due to concussive shock waves due to blasts [7].

### 1.2.3 Components of a Sports Helmet

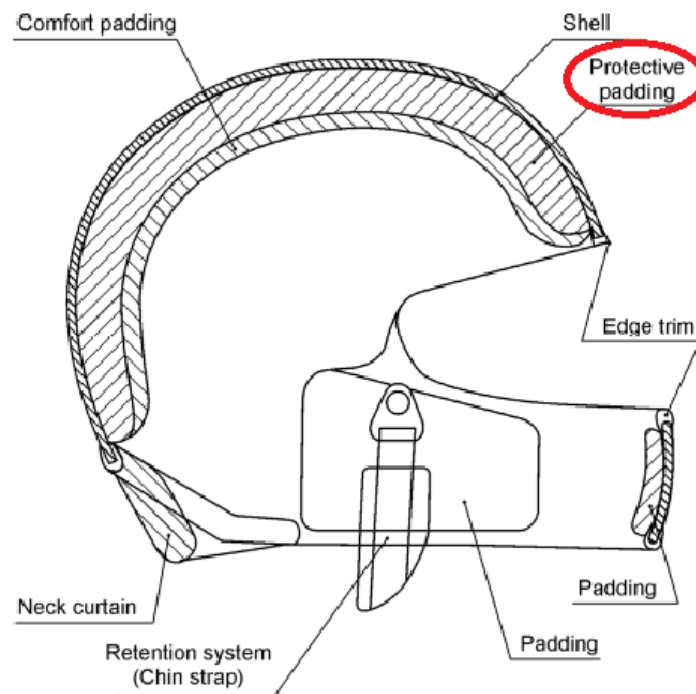


Fig. 1.4. Cross section of a helmet with names of different components.

- Outer hard shell

This is the outermost layer of the helmet. It is very thin and should be robust to sustain the incoming impact forces. The outer shell is generally made up of

a tough plastic material. Average thickness of this shell is in between 1 to 2 mm. It should also have a high fatigue life and a high fracture strength.

- Protective padding

This is the layer which absorbs substantial energy. It is generally made up of viscoelastic foam. Most of the modern helmets like Riddell football helmets have Vinyl Nitrile foams. The information about these advanced foams is not completely disclosed by the helmet manufacturers. Hence, complete details about the composition and mechanical properties is not available in the literature. As stated earlier, some of the ordinary foams used in sports helmets are: Expanded Polypropylene foam, Expanded Poly Ethylene foam, etc.

- Comfort padding

It is a very low density foam arranged to give maximum wearing comfort to the head. It provides fit. These foams are generally memory foams. The residual stress remains for a considerable time after removal of the load. Comfort foam does not absorb much of the impact energy as compared to the protective padding. It has average thickness of around 3-5 mm.

- Other accessories

Helmets have other accessories like front shield, chin strap, neck curtain, etc. depending on the application. Front shield protects the face from frontal direct forces. Some modern football helmets have helmet mounted displays and radio communication.

While designing the components and entire helmet system, a consideration is given to the dissipation of heat. However, for this thesis it is considered as an out of scope factor and recommended as a future work.

### 1.2.4 Measurement of Helmet Performance

Helmet impact tests are performed using dummy headforms. Three parameters are measured from these tests which are: (1) Head Injury Criterion (HIC), (2) Peak linear acceleration, and (3) Peak rotational acceleration [8].

HIC is defined as:

$$HIC = \left\{ \left[ \frac{1}{t_2 - t_1} \int_{t_1}^{t_2} a(t) dt \right]^{2.5} (t_2 - t_1) \right\}_{max} \quad (1.1)$$

where,  $a(t)$  is the acceleration as a function of time measured in standard gravity acceleration and  $t_1$  and  $t_2$  are initial and final times respectively. Maximum time ( $t_2 - t_1$ ) is selected between 3 ms to 36 ms, usually it is taken as 15 ms [9]. Peak linear acceleration is also measured in terms of standard gravity (g) and peak rotational acceleration is measured in  $rad/s^2$ . When value of HIC is 500, then there is 5% risk of the head injury. Among some other criteria are femur load and chest injury.

### 1.3 Shortcomings of the Existing Designs

Some of the current studies say that existing helmets are not safe enough to prevent players from concussions [10]. An extensive research has been done on the foams for their application in helmets [11–15]. Although foams absorb energy they are not protective enough to provide the protection from TBI. There are mainly two shortcomings of the liner foams.

1. They fail under high strain rates. When foams are subjected to high strain impacts they behave similar to a stiff material. The energy dampening is hampered. Hence, they fail to provide the protection [16].
2. Foams do not provide protection from rotational forces. Studies show that helmets do not have the required capability to keep the acceleration and strain on the brain within limits [16].

#### 1.4 Recent Developments and Non Traditional Energy Absorbing Structures Used in Modern Helmets

Advancement in technology has widened the scope of research on energy absorbing structures. Non-traditional solutions other than foam are emerging in recent years. Following are some of the commercial helmets which have non-traditional designs. Schutt and Zenith manufacture football helmets whereas 6d is a motorbike racing helmet manufacturer and Smith optics helmets are bicycle helmets.

- TPU cushioning - Schutt helmet

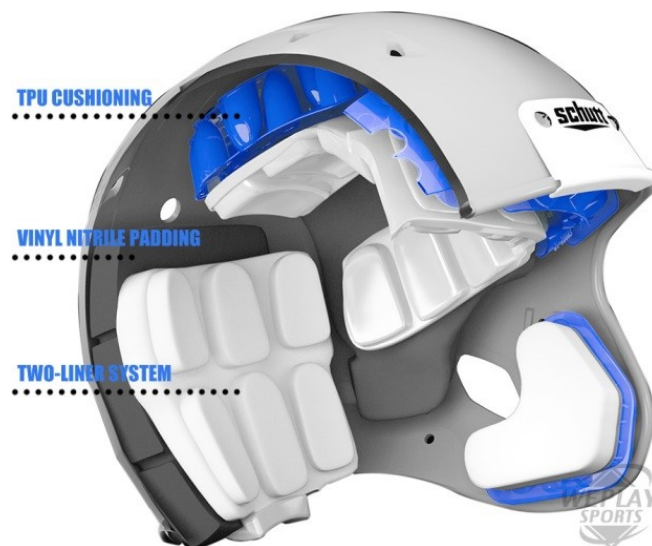


Fig. 1.5. Section of a Schutt DNA helmet showing TPU cushioning and other parts  
(Source: <https://www.schuttsports.com/science-of-domination>).

Multiple series of helmets from Schutt sports have Thermoplastic Polyurethane (TPU) cushioning in it. TPU cushioning was originally introduced by Schutt in 2003 in Schutt DNA pro helmet. Some lab tests have proved that TPU cushioning provides better protection and it especially works well at the temperature range found in actual game conditions i.e at the temperature of 115-120 degrees. It is claimed that TPU cushioning also provides better hygienics. These hel-

mets are reportedly replacing the existing traditional helmets with foam. This helmet is as shown in Figure 1.5.

- Air shock absorbers - Xenith helmets



Fig. 1.6. Zenith helmet with air cushioning for energy absorption (Source: <http://www.xenith.com/pages/xenith-technology>).

A Michigan based helmet company Xenith, uses air cushioning in their helmets. These helmets have a shock bonnet for energy absorption. Shock bonnet consists of a number of air shock absorbers. The design of these shock absorbers is patented by the company. Xenith claims that these helmets adapt to the impact forces. As a result the outer hard shell has an independent movement which provides better protection. This helmet is as shown in Figure 1.6.

- Omni-Directional suspension system - 6d helmet

6d helmets makes motorcycle helmets. The use of EPS foam is not completely eliminated from these helmets. For energy absorption, EPS foam is still implemented. As marketed by the company, in addition to the energy absorption





Fig. 1.7. A 6d helmet with omni directional suspension system implemented together with EPS foam  
(Source: <http://www.6dhelmets.com/innovation/>).

the design of this helmet is focused on reducing angular acceleration on head. There are two layers of EPS foam. These two layers are connected by an array of 27 elastomeric Isolation dampers which have progressive spring rate. These dampers have unique hourglass shape. They are omni-directional meaning that they can have movement in all directions including linear and rotational movement. In other words, they have total of six degrees of freedom. Hence, the name of the company is 6d. Elastomeric Isolation Dampers provide relative movement between the two layers of EPS foam. Hence, angular forces on the head are reduced as claimed by the company. This helmet is as shown in Figure 1.7.

- Koroyd-EPS system - Smith optics helmet

Smith Optics has introduced a new material system for impact protection called as Koroyd. Koroyd consists of thousands of co-polymer extruded tubes which are like straws. The helmets introduced by Smith optics use Koroyd in com-



Fig. 1.8. Smith optics Koroyd straws helmet  
(Source: <http://www.smithoptics.com/us/techhelmet>).

combination with EPS foam. Energy is absorbed by EPS foam as well as Koroyd. Upon impact, the cores of Koroyd crush in a controlled manner decelerating the energy from the impact and reducing trauma levels as claimed by the company. Smith optics helmets are used as bicycle helmets. It is as shown in Figure 1.8. It is also claimed that the design of this system has a good air circulation.

- D30 trust helmet pad system

D3O materials flow freely in their raw state when moved slowly, but on shock, lock together to absorb and disperse energy, before instantly returning to their flexible state. This reaction is counter intuitive. Greater the force of the impact, more the molecules lock together and greater is the protection. It is a British innovation based on nanotechnology. It is claimed that the impact protective behavior of the material is dependent on the impact velocity.

## 1.5 Proposed Solution

In this research we propose a layered cellular composite structure which has three layers. The main idea is to divert the incoming impact forces in the radial directions



Fig. 1.9. D3O trust helmet pad system (Source: <http://www.d3o.com/>).

which are normal to the direction of the impact. This idea is first proposed by Gokhale et al. [17]. The primary concept is as shown in the Figure 1.10.

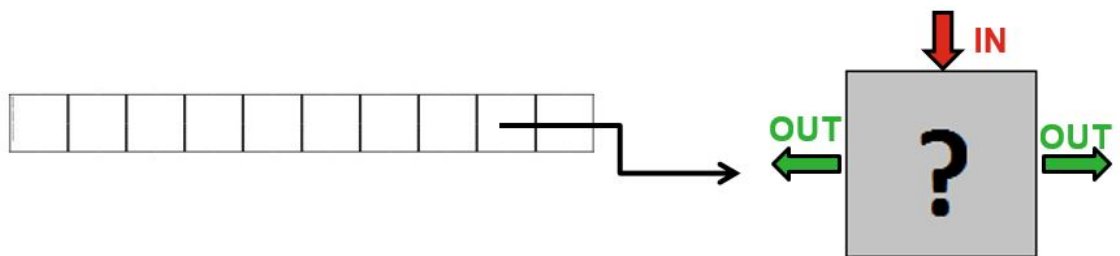


Fig. 1.10. Concept of the proposed solution.

### **1.5.1 Outer Hard Shell**

This is the topmost layer. It should be light-weight and stiff with high yield strength. It can be made up of a fiber woven composite imbided in a polymer matrix. It should distribute the incoming impact forces over the second layer and provide robustness to the structure.

### **1.5.2 Compliant Buffer Zone (CBZ)**

This layer is sandwiched between top and bottom layers. It is responsible for dampening of the most of the impact energy. Hence, design of this layer is very crucial. It should implement something that diverts the incoming impact forces in multiple radial directions to have maximum energy absorption capacity. We propose that the function of diverting forces should be completed using an array of several compliant mechanisms.

### **1.5.3 Inner Layer**

It can be a cushioning or a hard plastic or metal layer depending upon the application. It should establish the contact between two adjacent layers.

## 2. DESIGN PROCEDURE

### 2.1 Design of Compliant Mechanism

A compliant mechanism is a structure that can transfer energy, force and displacement from one point to another point. Compliant mechanisms are different than rigid mechanisms in many ways. In rigid mechanisms several links are connected at joints but relative motion between the links is restricted. Energy is conserved between input and output ports if friction losses are neglected. Such mechanisms do not perform work. Unlike rigid mechanisms, compliant mechanisms have at least a few flexible members.

Compliant mechanisms gain at least some of their mobility from the deflection of the flexible members. Due to the inclusion of flexible members compliant mechanisms can store energy in the form of the strain energy. Hence, these mechanisms might be suitable for the development of the concept of the ALC. The use of compliant mechanism for the applications in energy absorbing structures has been demonstrated at the research level [18–20].

There are many methods of designing compliant mechanisms. The most famous methods are: (1) Pseudo rigid body model (PRBM) method, (2) Optimization methods, and (3) Inverse analysis [21]. In PRBM method, different types of flexible components are assigned with different pseudo rigid models. These models are used to convert flexible member to equivalent rigid member who have similar force-deflection characteristics. After that rigid link mechanism theory can be used for the analysis of compliant mechanisms. Many researchers have worked on this method [22–27].

Continuum optimization methods are also used for designing compliant mechanisms. Generally, these methods have a common basic definition of the problem: minimize an objective function  $f(x)$ , under a set of boundary conditions by varying

the value of one or more design variables  $x_j$  within the specified bounds [21]. In mathematical form this problem can be stated as :

$$\begin{aligned} \text{Minimize} \quad & f(x) \\ \text{Subject to:} \quad & g_j(x) \leq 0; j = 1, 2, \dots, m \\ & h_k(x) = 0; k = 1, 2, \dots, m \\ & x_l \leq x_i \leq x_u \end{aligned}$$

where,  $g_j$  are inequality functions,  $h_k$  are equality functions and  $x_l$  and  $x_u$  are lower and upper limits for the design variable  $x_i$ . There are three levels of the continuum optimization which are: size, shape and topology optimization.

Inverse methods are aimed at finding the initial shape of the beam such that, under the service loads initial shape of the beam is converted into the final design shape [28,29]. This concept is currently in the development stage and some drawbacks are pointed out for this method. Work is going on to create the automatic design tools using inverse methods.

For our work we selected topology optimization method for designing compliant mechanisms as it is the most advanced method present today.

### 2.1.1 Topology Optimization

Topology optimization is a Mathematical approach to optimize a material layout in a given space. It is the most general form of the structural optimization. It is used at the concept level of the design process. Topology optimization has a significant contribution in the design of energy absorbing structures [30–35]. Topology optimization of helmet liners or any other components of helmets is not explored much. However, design of vehicle components like thin walled tubular structures using topology optimization is area of focus for many research groups all over the world [36–39].

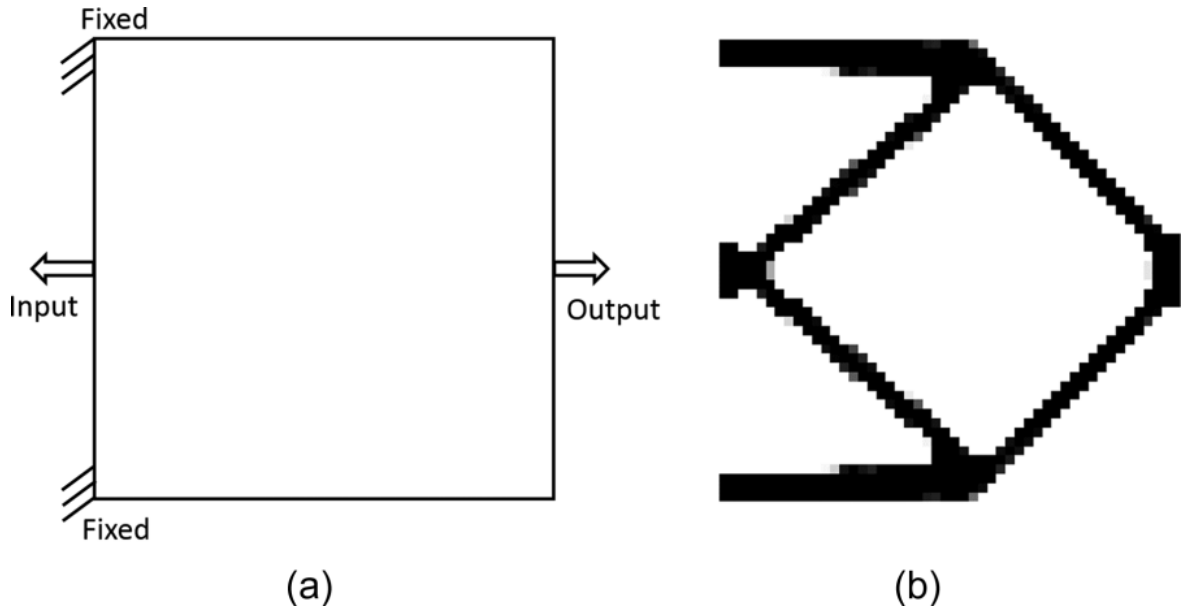


Fig. 2.1. Classic force inverter compliant mechanism (*C.H. Liu, G.F. Huang, "A Topology Optimization Method With Constant Volume Fraction During Iterations for Design of Compliant Mechanisms", J. Mechanisms Robotics, vol.8, no. 4, 2015*).

Ananthasuresh, G.K. first introduced the structural optimization of the compliant mechanism by adapting the homogenization method and using the displacement of one point in the mechanism as the objective function [40]. A lot of research has been done on the topology optimization of compliant mechanism after that [41–46]. Figure 2.1 shows topology optimization of a classic force inverter compliant mechanism.

## 2.2 Conceptual 2D Design of Compliant Mechanism

### 2.2.1 Numerical Formulation

The objective of the topology optimization of the compliant mechanism is to obtain a maximum displacement at the output port. The numerical formulation can be stated as follows:

$$\begin{aligned}
 &\text{Find} && \tilde{x} = [x_1, x_2, \dots, x_i, \dots, x] \\
 &\text{Minimize} && c(\tilde{x}) = -u_{out}(\tilde{x}) = -L^T U(\tilde{x}) \\
 &\text{Subject to} && v(\tilde{x}) = x^T v - \bar{v} \leq 0 \\
 &&& x \in X, X = \{x \in R^n : 0 \leq x \leq 1\}
 \end{aligned}$$

where,  $L$  is a unit length vector with zeros at all degrees of freedom except at the output point where it is one and  $U(\tilde{x}) = K(\tilde{x})^{-1}F(\tilde{x})$  [47].  $\bar{v}$  is called as volume fraction. It limits the maximum amount of the solid material in the design. Chosen value of the volume fraction is proportional to the mass of the final structure. An optimum value should be selected for getting the lightest structure with the desired strength. There are other parameters which should be manually selected like filter radius and penalization factor. These factors are chosen as suggested in the literature [48].

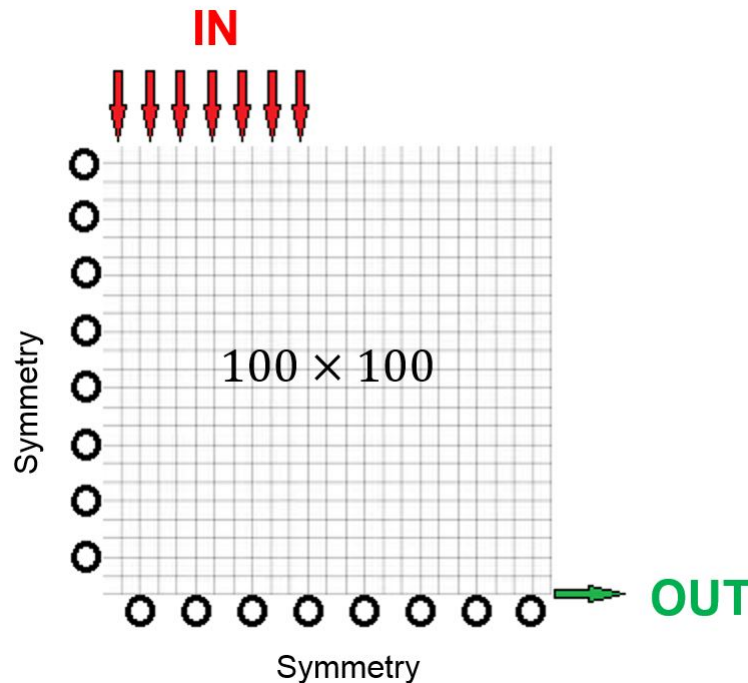


Fig. 2.2. Initial design domain, loads and boundary conditions used for 2D topology optimization of compliant mechanism.



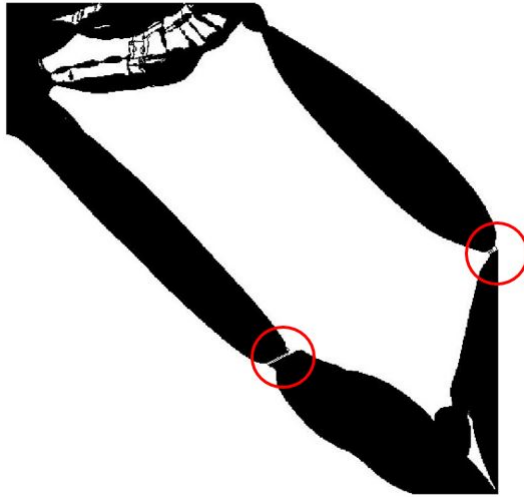


Fig. 2.3. Result of single material topology optimization.

Figure 2.2 shows the initial design domain with loads and boundary conditions. Two dummy load cases are considered at the input and the output ports in the form of springs. These springs add a stiffness and an external force at the the input and the output nodes. Initial design domain is of the size  $100 \times 100$ . There are multiple input ports in the left half of the top edge. The output port is set at the bottom right corner. A uniformly distributed load is applied at the input port which is directed downwards. The desired displacement at the output port is in the right direction. The Solid Isotropic Material with Penalization (SIMP) approach is used for optimization which was initially proposed by Bendsøe [49].

Only two regions are considered. One is a solid region with material and the other one is a void. For avoiding the checkerboard pattern and getting a binary result a very small filter radius equal to 1.0 is selected. The result of the topology optimization is as shown in Figure 2.3. Two thin hinges are produced.

### 2.2.2 Problems Due to Thin Hinges

Due to extremely tiny hinges of the compliant mechanism, two problems occur. First problem is that, the CAD model of the compliant mechanism is extremely difficult to replicate in the process of additive manufacturing. We printed a 2D compliant mechanism with a thickness and a revolved 3D compliant mechanism using a Stratasys uPrint 3D printer. The material used is Acrylonitrile Butadiene Styrene (ABS). The selected dimensions of the 2D compliant mechanism are  $25mm \times 25mm$  and value of the volume fraction  $\bar{v}$  is 0.3. But even for this scale of the compliant mechanism the size of the hinges are not compatible with the resolution of the printer. It is also found that the support material at the hinges is not completely removed when kept in the solution bath for a time of more than 12 hours. Due to these problems, the desired movement of the compliant mechanism is not obtained. The 3D printed compliant mechanism is shown in the Figure 2.4.

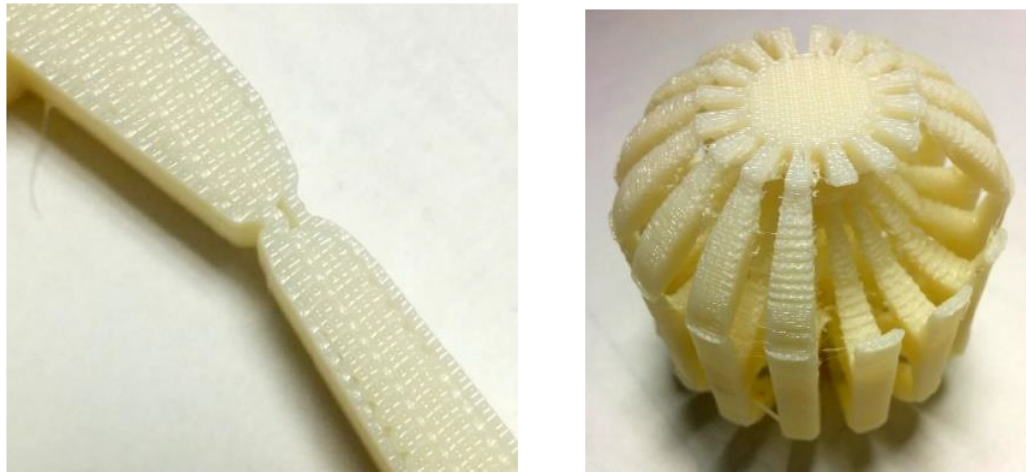


Fig. 2.4. 3D printed compliant mechanism with only one material.

The second problem due to the thin hinges is the failure of the mechanism due to extreme stress concentration. We performed a 2D transient finite element analysis

using LS-Dyna on the obtained geometry. The hinges broke down as shown in the Figure 2.5.

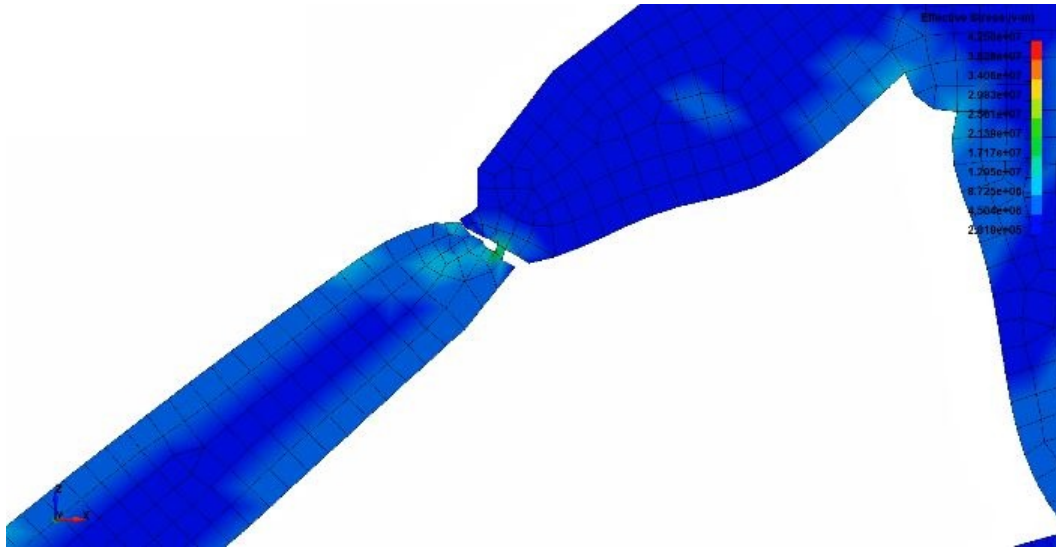


Fig. 2.5. Finite element analysis showing failure due to stress concentration.

Therefore, the compliant mechanism designed and optimized using this approach cannot be used to design the CBZ of the proposed ALC. Extremely thin hinges must be eliminated to ensure the strength and a high energy absorption capacity.

### 2.2.3 Multi-Material Topology Optimization of the Compliant Mechanism

The inclusion of multiple materials in the topology optimization process has the potential to eliminate the narrow, weak and hinge-like sections that are often present in single-material compliant mechanisms. Compliant mechanisms designed using multi-material topology algorithms also produce more displacements [50]. A 115 lines matlab code was written by Tavakoli et al in 2014 using an alternating active-phase algorithm for multi-material topology optimization problem [51]. This code is a modified version of the 88 lines matlab code for single material by Andreassen et al. [48].

In case of multi-material topology optimization there are multiple volume fractions related with each material phase. The admissible design space can be given as:

$$A_{ab}^h := \left\{ \alpha_a^h \in v^h \mid l_a^h \leq \alpha_a^h \leq u_{a,temp}^h, \int_{\Omega^h} \alpha_a^h dx = \Lambda_a |\Omega^h| \right\} \quad (2.1)$$

where,  $\alpha$  is the vector of the volume fractions with components equal to the number of phases. The value of the volume fraction corresponding to each phase varies between an upper limit and a lower limit. The summation of all the volume fractions must be equal to one in order to avoid gaps or overlaps [51].

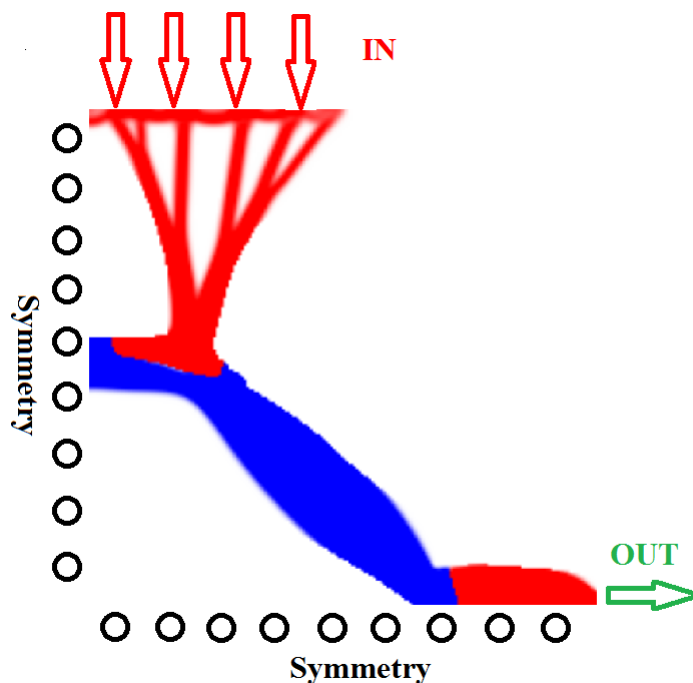


Fig. 2.6. Result of multi-material topology optimization of the compliant mechanism.

Total three phases are considered which consists of a rigid material phase, a flexible material phase and a void. Hence for this problem,  $p = 3$ . The rigid material provides the strength and the flexible material is helpful for generating the desired displacement. The result after performing topology optimization is as shown in the Figure 2.6. It can be seen that the tiny hinges are completely eliminated in this design.

In this case the selected filter radius is 5.0. Even though this radius is comparatively large than the previous one, the result is completely free of the checkerboard pattern. All the phases are clearly separated. Increased filter radius is the main reason behind the elimination of the thin hinges.

The branches at the top portion are neglected because these can be eliminated if the numbers of iterations are reduced. After a certain number of iterations the algorithm starts reducing the material present in the top region of the rigid material considering the problem as a case of minimizing the compliance. Hence, various branches are produced.

### 2.3 3D Compliant Mechanism

Using CAD tools, the 2D compliant mechanism is converted to an axis symmetric 3D compliant mechanism. Some other changes are made by adding and removing some material in order to make it suitable for additive manufacturing. This mechanism has six output ports at the mid-height as shown in Figure 2.7.

To analyze the behavior of the compliant mechanism, a transient finite element analysis is performed. A constant load of 10 N is applied on the top surface which is the input port of the compliant mechanism. All the nodes at the bottom surface are fixed. The graph of input displacement vs output displacement is as shown in Figure 2.8. From this graph, the ratio of the output displacement to the input displacement which is also known as Geometric Advantage is approximately equal to 0.25.

From another graph of force vs displacement as shown in Figure 2.9, the spring constant of the compliant mechanism,  $K \simeq 1000 \text{ Nm}$ .

### 2.4 Design of Connections Among Compliant Mechanisms

Several compliant mechanisms are arranged in an array and they should be connected among themselves. The pattern of the compliant mechanisms in the array is selected such that output ports face each other. Connections among compliant

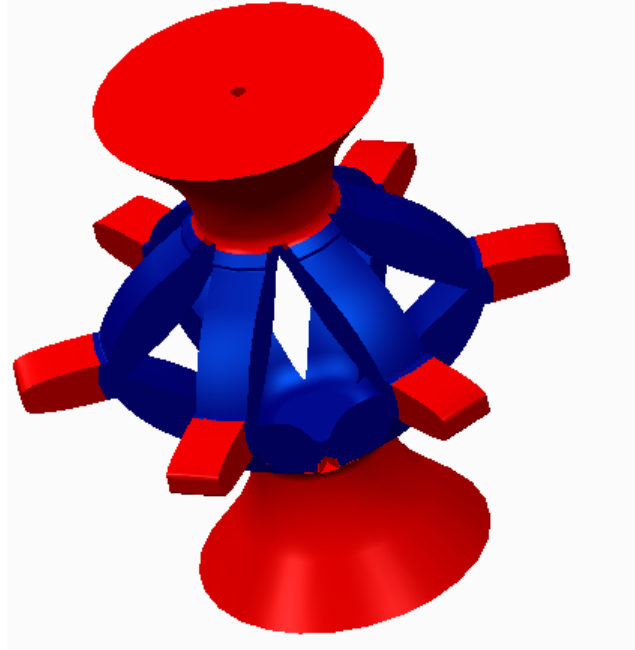


Fig. 2.7. 3D axis symmetric compliant mechanism.

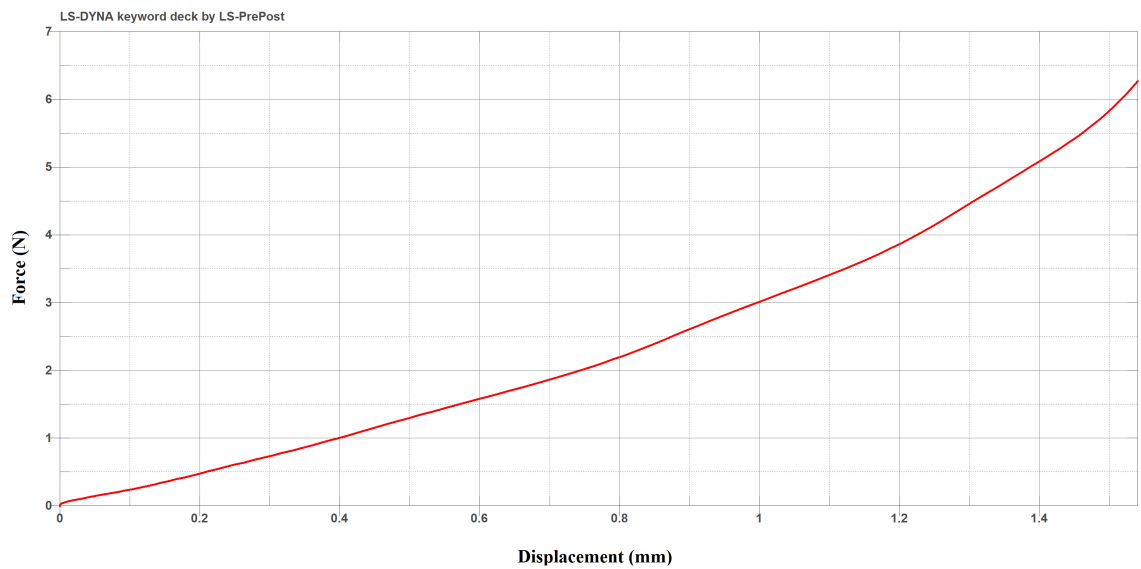


Fig. 2.8. Input displacement vs output displacement of 3D compliant mechanism.

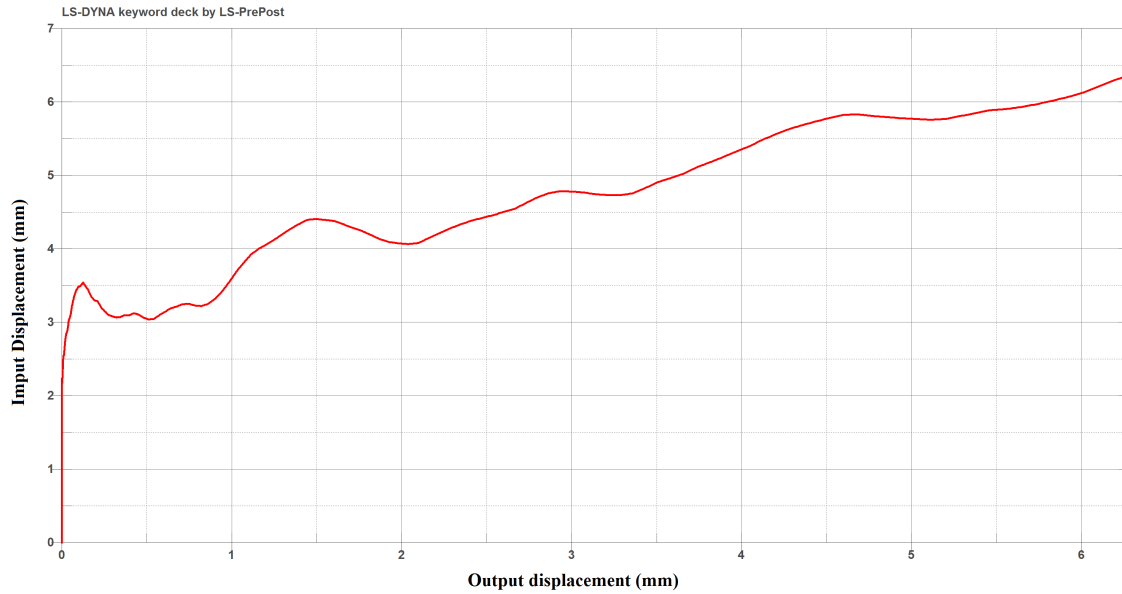


Fig. 2.9. Force vs displacement graph for 3D compliant mechanism.

mechanisms are designed to absorb the impact energy when they are compressed due to the displacement of the output ports of compliant mechanisms. Another function that these connections owe is to reduce forces on the head when an oblique impact occurs. The requirement for achieving both the objectives is that, connections should have a spring action.

The ideal choice is the use of coil springs. However, the ALC is supposed to be manufactured using additive manufacturing. Additive manufacturing of the coil springs is not recommended. The main reason behind this is that, coil springs are at a very high risk of breaking due to a small coil diameter during the high pressure post-processing for removing the support material. Additionally, coil springs consume more support material than the build material. Hence, some different design must be selected as connection among compliant mechanisms.

Another feasible option which is a rubber springs is used as a connection . The design of the rubber spring is as shown in the Figure 2.10. When an oblique impact occurs, connections provide the flexibility such that some rubber springs act in tension



Fig. 2.10. Flexible rubber spring for connecting compliant mechanisms.

and others in compression depending on their relative position with the impact point and the direction of impact. This allows a relative movement between outer and inner layers.

Some gaps are created to make a way for removal of the support material. Overall height of the ALC is 27 mm and that of CBZ is 25 mm. Outer diameter of each compliant mechanism is also 25 mm. Rubber spring has a mean diameter = 5 mm, pitch = 1.9 mm, thickness = 0.5 mm and length = 10 mm.

A transient Finite Element Analysis test similar to the previous test for 3D compliant mechanism is performed on the rubber spring. In the simulation it is seen that the gaps in the rubber spring do not affect its compression process and no stress concentration is observed. The rubber spring is compressed progressively with a uniform deformation in each corrugation. This proves the suitability of this design as an energy absorbing structure. The graph of force vs displacement is as shown in Figure 2.11. Spring constant for the rubber spring is calculated as,  $K \simeq 500Nm$ .

## 2.5 Design of Complete ALC

Complete ALC looks like as shown in the Figure 2.12. Its working is summarized as follows. The outer hard shell directly comes in contact with the impacting object.



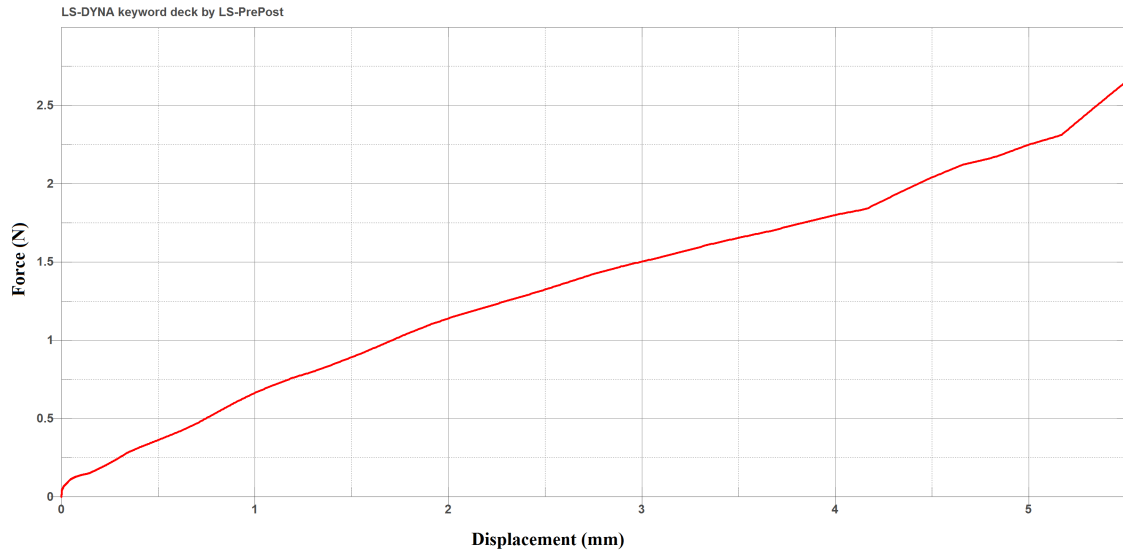


Fig. 2.11. Graph of force vs. displacement for the rubber spring.

It distributes the impact load along the input ports of several compliant mechanisms. Compliant mechanisms divert impact forces in radial directions normal to the direction of the impact. While doing so they absorb a portion of the impact energy. Remaining energy is dissipated in rubber springs which prove to be the ultimate sink of energy.

## 2.6 Conceptual Design of Helmet Using ALC

This section explains the conceptual design of a helmet using ALC. As compared to the traditional design there is lesser need of assembly for this design. Entire ALC can be made as a single unit.

### 2.6.1 Inner Comfort Foam

This is a layer similar to that present in the traditional helmets. Very low density Expanded Polyurethane (EPU) foam can be used as a comfort foam. The average

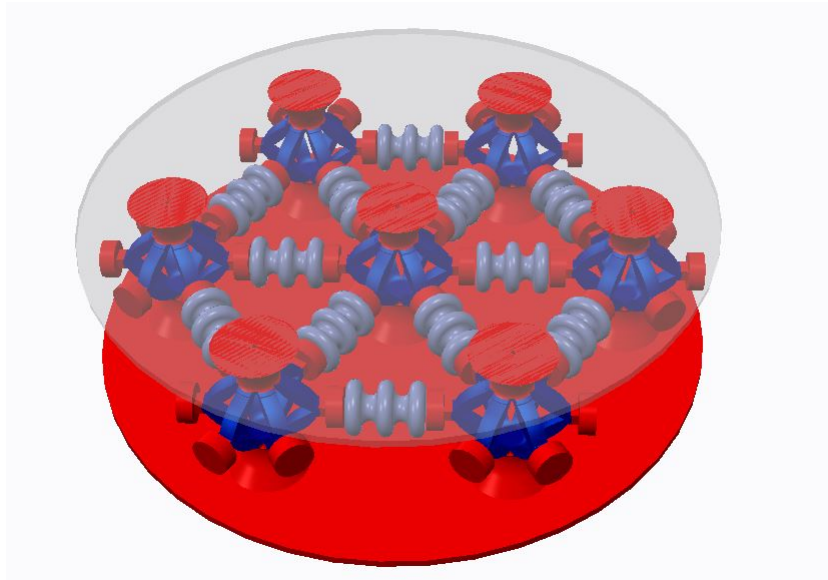


Fig. 2.12. Complete design of ALC.

layer thickness in this design is 4 mm. Some holes are provided so as to accommodate the threaded screw and holes for assembly. The comfort foam is as shown in the Figure 2.13.

### 2.6.2 ALC Within the Helmet Material System

The design of ALC has three layers as explained earlier. The thickness of the outer hard shell in this conceptual design is 1.5 mm and that of the bottom layer is 0.5 mm. The height of the compliant mechanism is 25 mm and diameter of each compliant mechanism is also 25 mm. It is as shown in Figure 2.14. The circles in the blue color are the input ports of the compliant mechanisms.

### 2.6.3 Front Protective Shield

The front protective shield is designed similar to the conventional design. It can be manufactured using traditional techniques or by additive manufacturing. Production

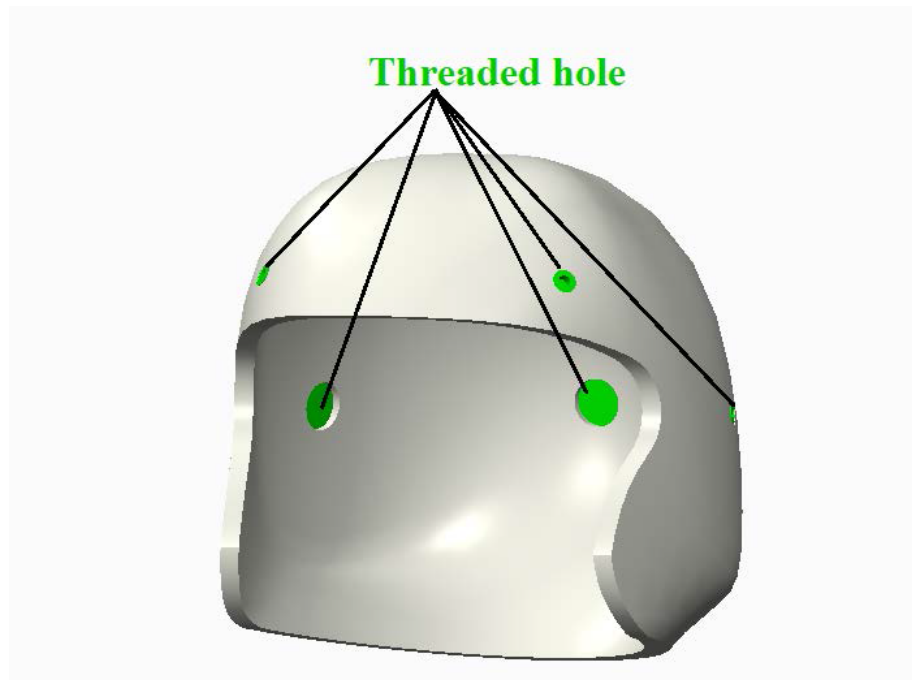


Fig. 2.13. The innermost comfort foam with slots for the threaded holes.

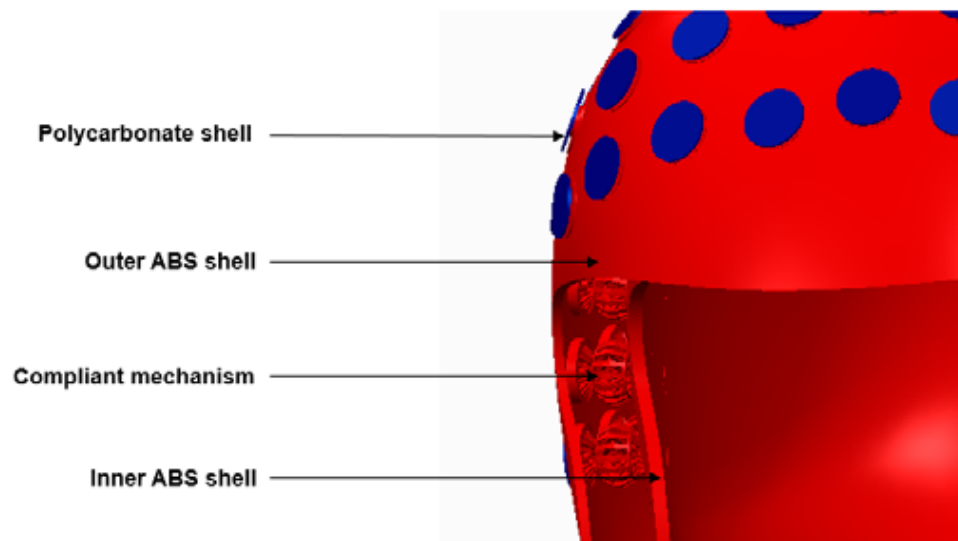


Fig. 2.14. The CAD model of integrated ALC with representation of different regions.

of the front protective shield can be integrated with ALC if it is given consideration while designing the CAD files for ALC. Doing so can reduce the assembly and the strength of the front protective shield.

The complete design of a conceptual helmet is as shown in the Figure 2.15

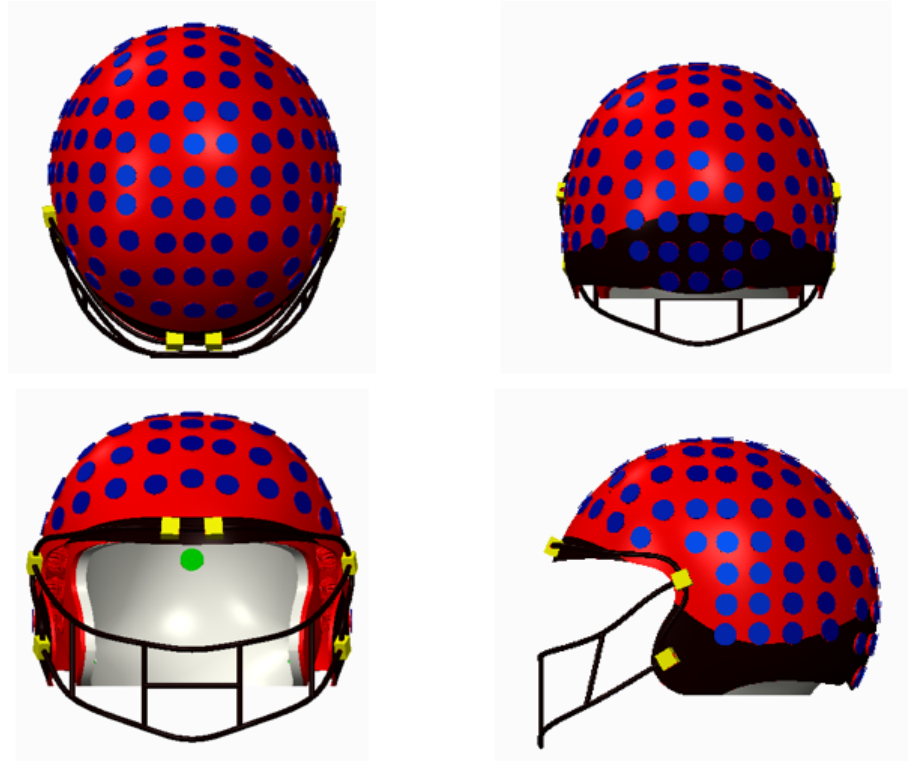


Fig. 2.15. Conceptual design of a helmet using ALC.

## 2.7 Polyjet Additive Manufacturing Technique

Polyjet additive manufacturing process is one of the most advanced processes existing today. Its working is similar to that of an inkjet printer. Instead of jetting drops of ink on a paper, polyjet 3D printers jet layers of curable liquid photopolymer onto a built tray. Figure 2.16 shows working of a polyjet 3D printer.

A liquid is used in the photopolymerization process which is radiation curable. These resins are also called photopolymers. Most photopolymers react to radiation

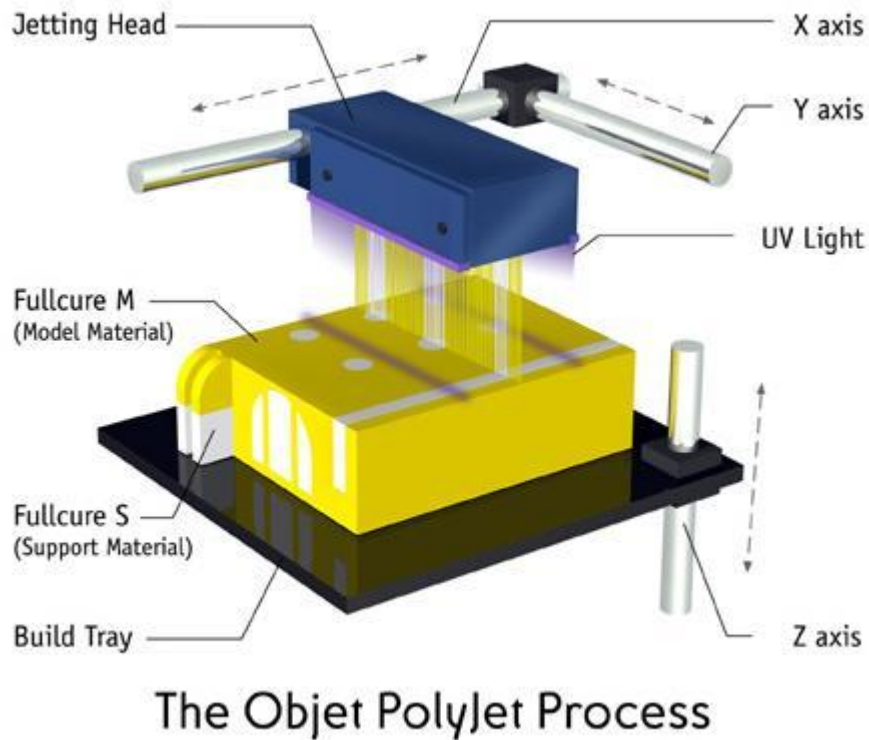


Fig. 2.16. Working of a polyjet 3D printer (<http://3dprinterblog.net/polyjet-3d-printing/>).

in the ultraviolet range of wavelengths. Sometimes visible light systems are used also. Upon radiation, photopolymers undergo a chemical reaction and are changed to solid state. This process is called photopolymerization, and is typically complex, involving many chemical participants [52].

There are three steps involved in the process of Polyjet printing. First step is the build preparation. This step involves placement of photopolymers and support material from a 3D CAD file. Software provided with the 3D printer automatically calculates the support material requirements. Second step is the production step. The 3D printer jets and instantly cures tiny droplets of liquid photopolymer. Fine

layers accumulate on the build tray to create parts. In the third step, the support material is removed using a solution bath or a high pressure solution jet.

Polyjet 3D printing creates smooth and detailed parts with high precision. This process achieves complex shapes, intricate details and delicate features. It easily incorporates a wide variety of colors and materials. A precision as fine as 16 microns can be obtained for smooth surfaces and complex objects.

## **2.8 Selection of Materials for Different Components of ALC**

This section describes the factors to be considered and material recommendations for different components of ALC.

### **2.8.1 Materials for the Top Hard Shell**

As stated earlier the recommended material for the top layer or the outer hard shell is a fiber woven composite reinforced in a polymer matrix. These composites are lightweight having an impact strength even greater than some of the metals. The most commonly used fibers are glass fibers. Glass fibers are comparatively cheap and provide high strength to the composite. However, for some applications these fibers are not strong enough. Carbon fibers are more costly, but provide more strength to the composites than the glass fibers. When there is no barrier of cost, ultra-high strength fibers like Kevlar<sup>TM</sup> or Spectra<sup>TM</sup> can be used. Applications of these fibers are currently limited to the use in aerospace industry and ballistic equipment. The matrices are generally epoxy resins or polyamides. Low cost option for the matrix is the use of unsaturated polyester/styrene.

If the budget is not enough for the use of even lowest cost composites, use of plastics like polycarbonate (PC) is recommended as a material for the top layer of hard shell. As the name suggests, these are polymers containing carbonate groups. It is a durable material and it also has a high impact strength. However, as it a glass like brittle material the scratch resistance is low. A layer of hard coating is applied

on it to improve the scratch resistance. Mechanical properties of PC are as given in Table 2.1.

Table 2.1  
Mechanical properties of polycarbonate.

<b>Property</b>	<b>Value</b>	<b>unit</b>
Density	1200-1220	kg/m <sup>3</sup>
Young's modulus	2.0 - 2.4	GPa
Elongation at break ( $\epsilon$ )	80-150	%
Poisson's ration( $\nu$ )	0.37	
Izod impact strength	600-850	J/m

Combination of PC with ABS are often used in practice. By varying the proportion of PC and ABS the cost and the strength can be varied.

## 2.8.2 Materials for the CBZ

### Rigid domain

For rigid domain in the compliant mechanism, the material need not be of very high strength. This material should be cost effective and suitable for additive manufacturing. The most commonly used material for additive manufacturing is ABS. The properties of ABS are as given in Table 2.2.

For polyjet manufacturing process there is a similar material which can be a substitute for ABS. It is called as VeroWhite by Stratasys. VeroWhite is opaque white in color. It is rigid and durable. It is capable of producing smaller parts with complex features. There are many versions of VeroWhite material with slightly varying properties.

Table 2.2  
Mechanical properties of ABS.

<b>Property</b>	<b>Value</b>	<b>unit</b>
Density	900-1500	kg/m <sup>3</sup>
Young's modulus	2.0 - 2.4	GPa
Typical injection molding temperature	204-238	°C
Poisson's ratio( $\nu$ )	0.35	

### Flexible domain

A hyperelastic material is suitable for the flexible domain of compliant mechanism and for the rubber springs. The rubber like flexible material used in Polyjet 3D printing is called TangoBlack. Like VeroWhite, TangoBlack material also has its variants with varying properties. These rubber like materials have very high elongation at break. Applications of TangoBlack include consumer goods, toys, automotive components, computer components, architecture, jewelry, medical devices, etc. The important properties of TangoBlackPlus material as stated in Stratasys' material datasheet are as given in Table 2.3.

Table 2.3  
Mechanical properties of TangoBlackPlus.

<b>Property</b>	<b>Value</b>	<b>unit</b>
Polymerized Density	1140 - 1150	kg/m <sup>3</sup>
Tensile strength	1.8 - 2.4	MPa
Elongation at break	170-220	%
Compression set	0.5 - 1.5	%
Tensile tear resistance	2 - 4	Kg/cm



The cost of TangoBlack material is very high as of today. If an alternative process to additive manufacturing is found out, it will be wise to use a general hyperelastic material like Neoprene rubber, Nitrile rubber or Silicone rubber.

### **2.8.3 Material for the Inner Core**

The purpose of the inner core is to just provide support to the compliant mechanism and establish contact with the body in contact on the inner side of the helmet. Hence, any material that can save cost and suitable for additive manufacturing can be used. The first choice is always ABS. Considering its ability to be used in PolyJet printing, use of VeroWhite is beneficial.

### 3. PERFORMANCE ASSESMENT OF ALC UNDER IMPACT LOAD

In this section, the proposed ALC is compared with a traditional helmet structure for the calculation of performance measures which are directly responsible for the effectiveness of a structure in the application of protection from impact damage. The cross-section of a helmet is simplified in the form of a cylindrical sample. The liner foam is Expanded Poly-Polypropylene (EPP) foam which is very commonly used in the sports helmets. An impact test is performed which is simple, fast and easy to repeat. Non-linear explicit finite element analysis is performed using LS-DYNA with non-linear material models. LS-DYNA is an advanced general purpose multi-physics software package developed by Livemore Software Technology Corporation (LSTC). It is widely used for dynamic simulations all over the world. All the boundary conditions and impact loads are essentially same for both simulations in order to have a fair comparison.

#### 3.1 Test Setup

The test setup is as shown in Figure 3.1. Impacting object is a sphere having thickness 1 mm. The material of this sphere is polycarbonate. It has an impact velocity of 5 m/s. The impacting object is analogical to another helmet impacting the helmet under test. All the nodes at the bottom surface are fixed. A local co-ordinate system is placed at each of the output ports which are at the outer circumference. Local X-axes are along the motion of the output ports. Movement of these output ports is restricted along the local X-direction to consider the effect of other compliant mechanisms which are not considered in this setup, but are virtually present in the vicinity.

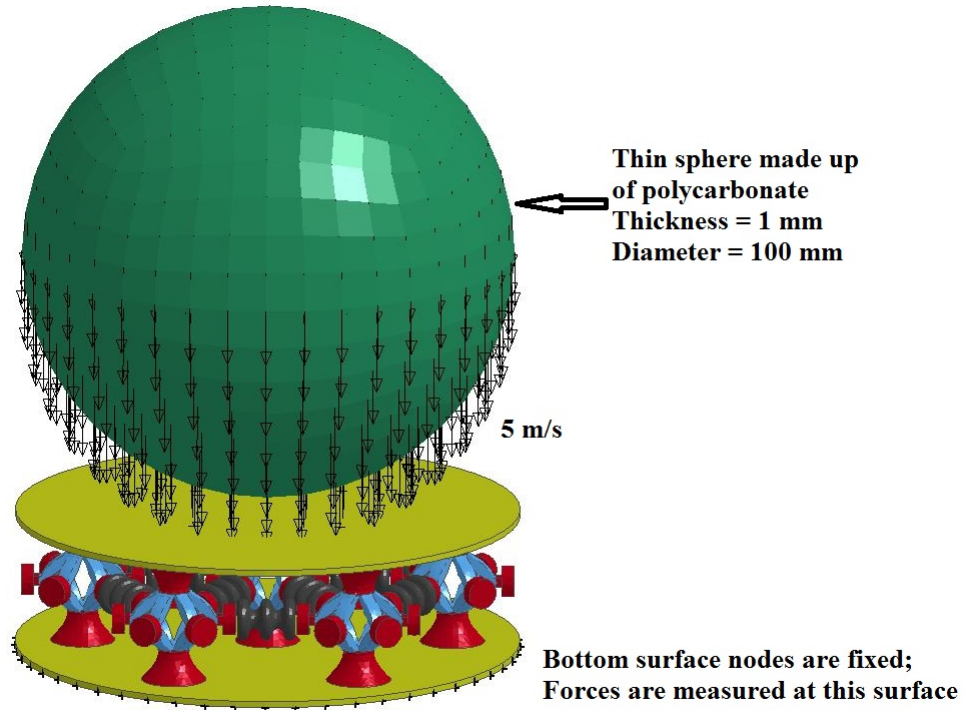


Fig. 3.1. Description of the test setup

Table 3.1  
Table about information of various element types used.

No.	Part	Element type
1	Compliant mechanism	Solid 4-noded tetrahedron
2	Top and bottom layers of ALC	Hexahedron
3	Rubber spring and impacting object	Belytschko-Tsay shell

Tables 3.1 and 3.2 give information about the element types used for meshing and the material models respectively. The shape of the compliant mechanisms is very complex. 4-noded tetrahedral elements are useful in conforming to the shape. Hence, these are used although their cost of calculation is more. Top and bottom

layers of the ALC are meshed using hexahedron elements. Polycarbonate sphere and rubber springs are of uniform thickness. Hence, the default shell formulation which is Belytsko-Tsay shell formulation is used for their meshing. The rubber spring shows uniform and true deformation as expected when meshed using shell elements.

Table 3.2  
Table of material density, elastic modulus and material models.

No.	Material	Density ( $kg/m^3$ )	Material model
1	Polycarbonate	1200	MAT024-PIECEWISE LINEAR PLASTICITY
2	ABS	1040	MAT024-PIECEWISE LINEAR PLASTICITY
3	EPP foam	86	MAT057-LOW DENSITY FOAM
4	NBR	1150	MAT027 MOONEY RIVLIN RUBBER

While designing the compliant mechanism, the input is supposed to be in the form of a uniform load in the downward direction only. In reality, the input load may not be uniform load and may be directed in any other direction. When the input load is varied, the performance of the ALC may also vary. Hence, the ALC is non-isotropic in nature. Therefore, in this work we have considered different possible cases of impacts. These are primarily divided as linear impacts and oblique impacts. In cases of linear impacts the direction of impact is parallel to the direction of the axis of compliant mechanism. In cases of oblique impact, the direction of impact makes a non-zero angle with the axis of compliant mechanism. Considering the geometry of the ALC, the case of linear impact can be further divided in three subcases with respect to the location of the impact. These subcases are as shown in the Figure 3.2.

In the first subcase, impact occurs exactly at the axis of one of the compliant mechanisms. In the second subcase the impact is offset from the axis and its location is at the midpoint of the line joining the two adjacent compliant mechanisms in the

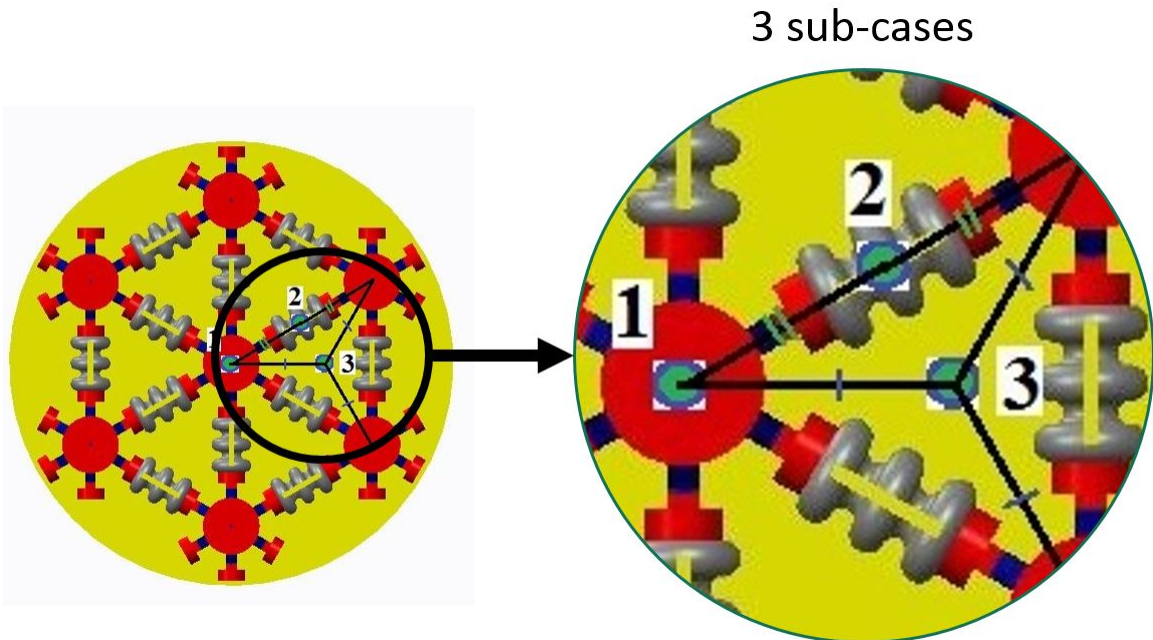


Fig. 3.2. Subcases of linear impact.

array. For the third subcase, the location of the impact is at the centroid of the triangle formed by three adjacent compliant mechanisms.

In case of oblique impact, two subcases are considered as shown in Figure 3.3. In two subcases impact is directed at  $30^\circ$  and  $60^\circ$  respectively with the axis of compliant mechanism. In these cases velocity of the object is also equal to 5 m/s. It has corresponding components in the vertical and horizontal directions.

Two parameters are observed in all the simulations which are kinetic energy of the impacting object and peak linear force at the bottom surface. From the graphs of the kinetic energy the time of contact can be found and it can be seen that how gradually energy is dissipated. Peak linear force transmitted from the bottom surface is analogous to the peak linear force on head if the ALC is considered as a part of a helmet. This force will be responsible for accelerations on the head. Analysis of these parameters for each subcase is given in the following sections.

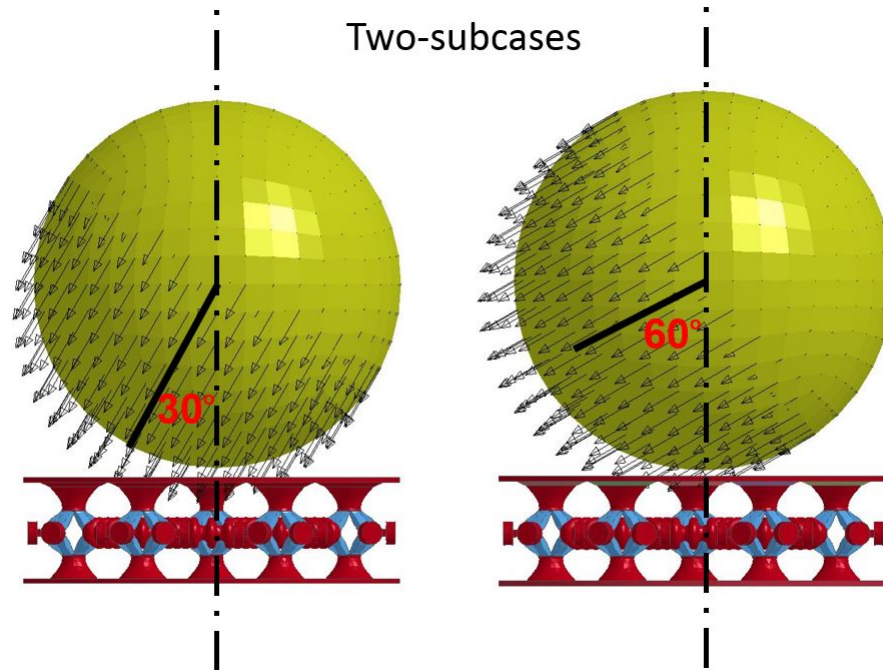


Fig. 3.3. Subcases of oblique impact

## 3.2 Results for Linear Impact

In this section, results for EPP foam and ALC are compared for linear impact. As the impact behavior of EPP does not change with the location of impact, it is tested only once.

### 3.2.1 Kinetic Energy

The curves of kinetic energy of the impacting object for EPP foam as well as different subcases of linear impacts are as shown in Figure 3.4. The red curve shows kinetic energy when EPP is used. Whereas, other curves in green, purple and blue colors are for the kinetic energy when the ALC is used. From this graph it can be seen that all of the kinetic energy is dampened in each case. However, the pattern of energy absorption is different for EPP and ALC. The contact between the object

and the protective structure is delayed when ALC is used. The location of the impact does not considerably affect the pattern of the energy absorption in case of ALC.

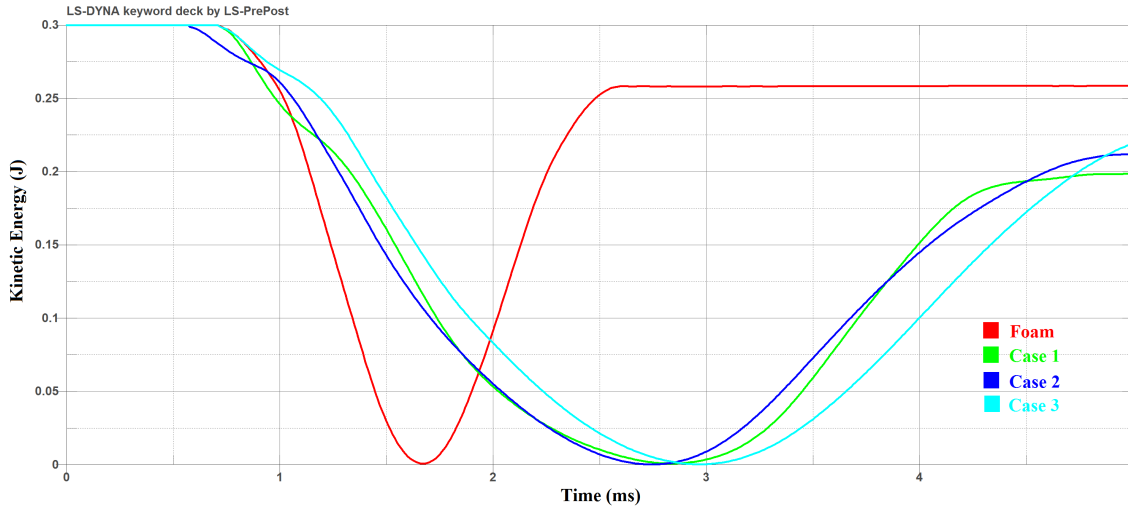


Fig. 3.4. Kinetic energy for subcases of linear impact.

Times of contact in each case are as given in Table 3.3. It is equal to 1.67 milliseconds (ms) when EPP is used. When the ALC is used the time of contact is 2.84 ms, 2.74 ms and 2.97 ms respectively for three subcases. If EPP foam is considered as the reference, then there is an increase of about 70% in all cases for ALC.

Table 3.3  
Time of contact for linear impact.

	<b>Foam</b>	<b>Case 1</b>	<b>case2</b>	<b>Case 3</b>
		<b>Axis</b>	<b>Midpoint</b>	<b>Centroid</b>
<b>Time of contact (ms)</b>	1.67	2.84	2.74	2.97
<b>Increase(%)</b>		70	64	77

### 3.2.2 Linear Force

Curves for the linear force in the direction of impact are as shown in Figure 3.5. Colors of the curves are same as used for the curves of the kinetic energy for the subcases of linear impact. The coloring scheme is also continued for all the results presented in the following sections. For the linear force the pattern of variation is different for EPP and ALC. However, this pattern does not vary much for different subcases of ALC. This observation is similar to the observation made for the graph of kinetic energy of the impacting object vs. time.

Values of the corresponding peak linear force are as given in table 3.4. The peak linear force is equal to 218 N for EPP and it is 108 N, 104 N and 99 N for different subcases of ALC. A decrease of around 50% is observed when the ALC is used in place of traditional EPP foam.

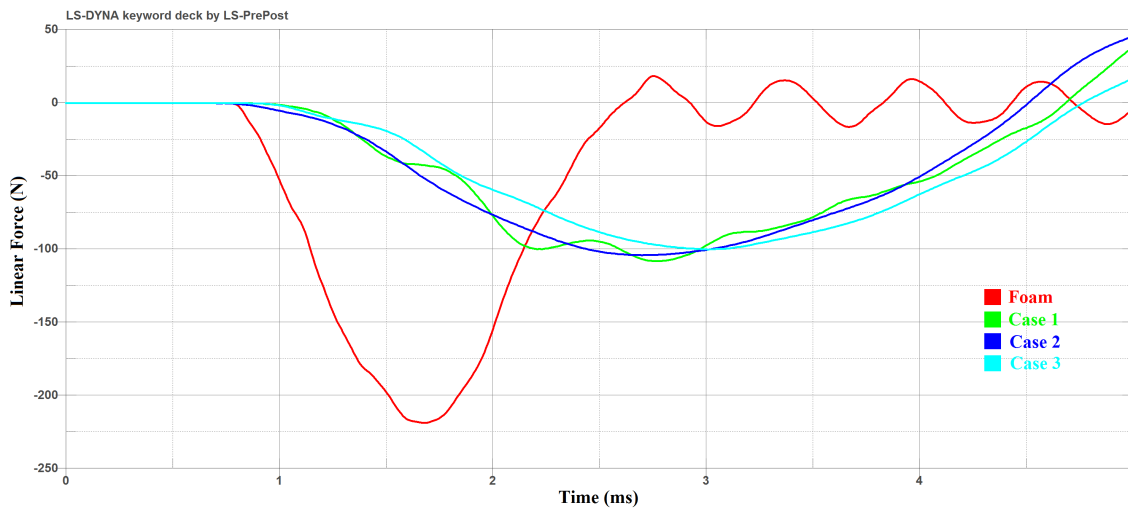


Fig. 3.5. Linear force for subcases of linear impact.



Table 3.4  
Peak linear force for linear impact

	Foam	Case 1 Axis	case2 Midpoint	Case 3 Centroid
Peak linear force (N)	218	108	104	99
Increase(%)		50	52	54

### 3.2.3 Max von Mises Stress on the Outer Hard Shell

The contours for von Mises stresses are as shown in Figure 3.6. Maximum von Mises stress when EPP is used is 10.28 MPa. For different subcases of the ALC, von Mises stress is respectively 9.61 MPa, 11.25 MPa and 12.65 MPa. It can be observed that, when the impact occurs exactly along the axis of compliant mechanism as in case 1, the maximum von Mises stress is decreased. But in rest of the two cases, it is more as compared to EPP foam. It can be easily inferred that the reason for this increase is that the distribution of the impact load is poor.

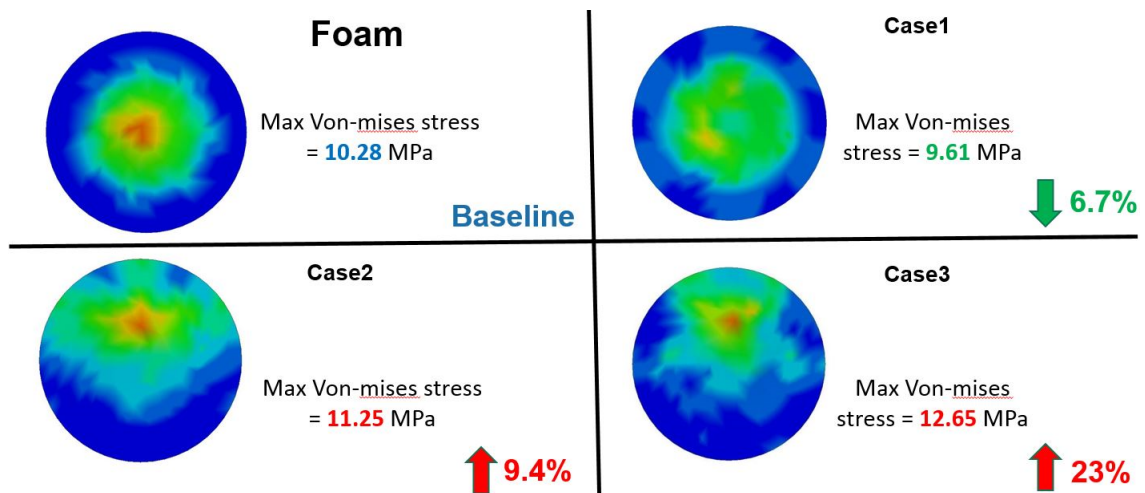


Fig. 3.6. Contours and maximum values of von Mises stresses on the outer hard shell for subcases of linear impact.

### 3.2.4 Maximum Strain on the Outer Shell

The material used for the outer hard shell is Polycarbonate which is not a ductile material. Hence, von Mises stress cannot predict the failure of the outer shell. Generally, failure criterion for glassy materials like Polycarbonate is the deformation [53]. But, in our case the deformation is difficult to measure directly. Another failure criterion which is elongation at break can also be considered as considered here. Elongation at break is the ratio of the change in length after breakage and initial length. It is also known as fracture strain.

Table 3.5  
Max strain (%) for subcases of linear impact.

	<b>Foam</b>	<b>Case 1</b>	<b>case2</b>	<b>Case 3</b>
		<b>Axis</b>	<b>Midpoint</b>	<b>Centroid</b>
<b>Max strain (%)</b>	47.48	47.22	54.34	60.21
<b>Increase(%)</b>		-11	15	27

We can predict the risk of failure of the outer hard shell by calculating maximum strain. Table 3.5 shows and compares values of mean strain produced. Mean strain is 47.48 % when EPP foam is used. It is equal to 42.22 %, 54.34 % and 60.21 % respectively for different cases of ALC. The variation is similar to the variation observed for von Mises stress. For the third case the increase in mean strain is around 27%. Hence, the third subcase should be considered as the critical case.

### 3.3 Oblique Impact

As stated earlier when EPP is used, the behavior of the simplified helmet structure is different for different impact angles. Hence, for each angle of impact under consideration, one simulation of EPP and one simulation of ALC should be done and then comparison should be held.

### 3.3.1 Kinetic Energy

Figures 3.7 and 3.8 show curves of kinetic energy vs time for EPP as well as ALC when impact occurs at  $30^\circ$  and  $60^\circ$  respectively. In both the cases kinetic energy is not completely dissipated by the simplified helmet structure. The energy absorption is almost the same in all the cases.

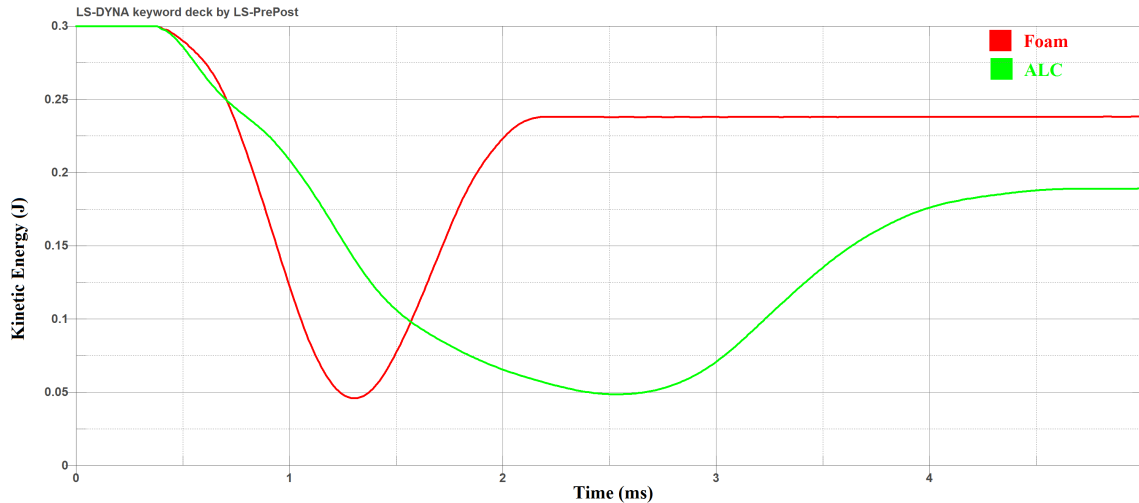


Fig. 3.7. Kinetic energy for oblique impact at  $30^\circ$ .

The values of time of contact are as given in Table 3.6. The time of contact is 1.31 ms for EPP and 2.54 ms for EPP and ALC respectively when impact occurs at  $30^\circ$ . It is 1.47 ms for EPP and 2.89 ms for ALC when impact occurs at  $60^\circ$ . Around 94% increase is observed for  $30^\circ$  and 97% increase is observed for  $60^\circ$  when ALC used.

### 3.3.2 Linear Force

Curves of linear force vs time for oblique impacts are as shown in Figure 3.9 and Figure 3.10 respectively for  $30^\circ$  and  $60^\circ$  impacts.

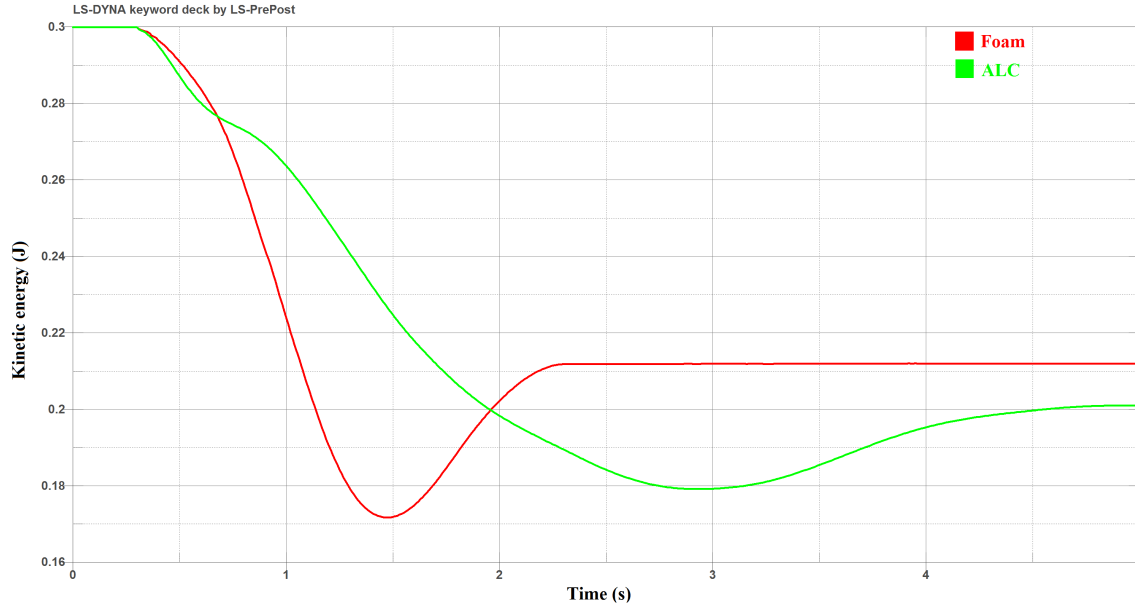


Fig. 3.8. Kinetic energy for oblique impact at 60°.

Table 3.6  
Time of contact for oblique impact.

	<b>FOAM</b>	<b>ALC</b>	<b>FOAM</b>	<b>ALC</b>
	30°	30°	60°	60°
<b>Time of contact (ms)</b>	1.31	2.54	1.47	2.89

The values of peak linear force for ALC and their comparison with EPP foam are given in Table 3.7. Around 50% decrease in the peak linear force is achieved when the ALC is used.

### 3.3.3 Max von Mises Stress on the Outer Shell

As shown in Figure 3.11, von Mises stress on the outer shell is increased when ALC is used instead of EPP foam. This increase is around 11% for subcase of 30°

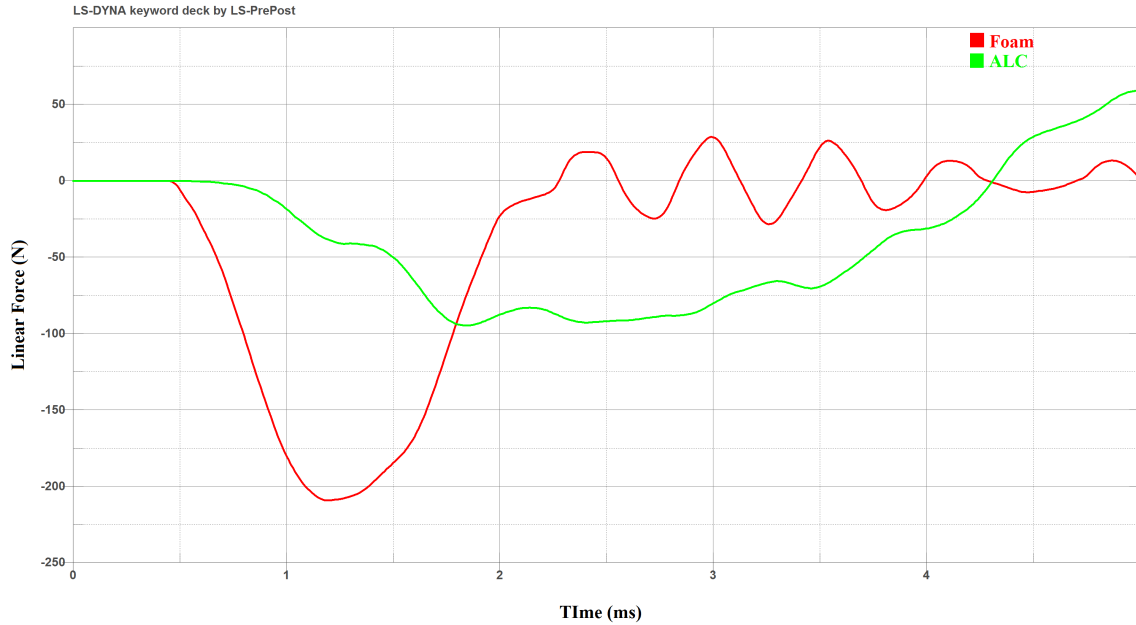


Fig. 3.9. Linear force for oblique impact at 30°.

Table 3.7  
Peak linear force for oblique impact.

	<b>FOAM</b>	<b>ALC</b>	<b>FOAM</b>	<b>ALC</b>
	30°	30°	60°	60°
<b>Peak linear force (N)</b>	209	95	112	58

and around 37% for 60°. But if the values of stress are considered, these stresses are comparatively less than those in case of the linear impact.

### 3.3.4 Maximum Strain on the Outer Shell

Values of maximum strain on the outer shell are as given in Table 3.8. Increase in the maximum strain recorded is around 44% when ALC is used for both the angles

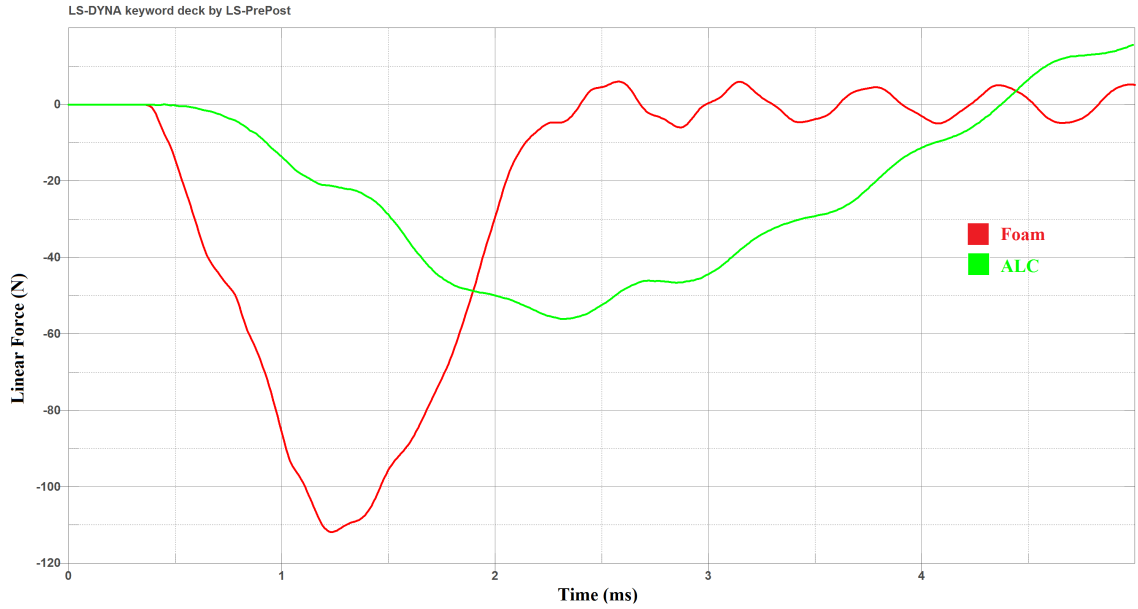


Fig. 3.10. Linear force for oblique impact at 60°.

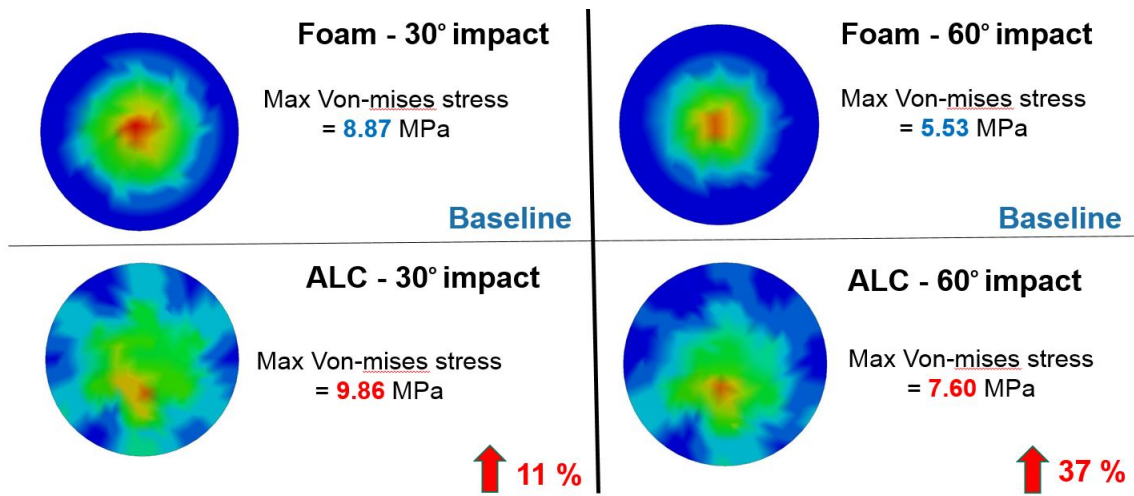


Fig. 3.11. Contours and maximum values of von Mises stresses on the outer hard shell for subcases of oblique impact.

of impact under consideration. However, the maximum value of the maximum strain is still less than that for the linear impacts. Hence, the third subcase of linear impact

that is when the impact occurs at the centroid of the triangle formed by three adjacent compliant mechanisms remains the critical case.

Table 3.8  
Max strain (%) for subcases of oblique impact.

	<b>FOAM</b>	<b>ALC</b>	<b>FOAM</b>	<b>ALC</b>
	30°	30°	60°	60°
<b>Peak linear force (N)</b>	36.89	53.37	35.61	50.92
<b>Increase(%)</b>		44		27

## 4. SUMMARY AND CONCLUSION

### 4.1 Summary

Foams are used in helmets for protection since decades. Literature reveals that, for improving protection capability of helmets some other solutions are required to be explored. There are some existing non-traditional commercial solutions that implement solutions other than foam. This work describes a new design of a helmet with an advanced layered composite structure which works through an array of compliant mechanism synthesis. A general design procedure is explained. This procedure can be used to design the impact absorbing materials of various sizes and quality by making appropriate changes in the geometry, dimensions and material properties. A simple impact test is carried out through a benchmark example in which a simplified helmet structure is subjected to normal and oblique impacts.

### 4.2 Conclusion

Performance of the ALC is examined by comparing it with the traditional EPP foam. The factors which are responsible for the linear and rotational forces on head are measured and compared. The results of this analysis show that ALC can give a good dampening performance under impact.

However, the failure of the outer hard shell is the identified critical factor which should be considered while designing a helmet using ALC. Attention should be given at achieving a required factor of safety for the outer hard shell.



### 4.3 Original Contribution

#### 1. Design of energy absorbing structure by diverting impact forces in radial directions

There are some previous attempts of developing impact diverting mechanisms. But, a completely novel concept of diverting impact forces through the use of an array of compliant mechanisms is presented in this thesis. This design concept is absent in the literature.

#### 2. Use of compliant mechanism and topology optimization tools for the design of helmet liners

The application of compliant mechanism and topology optimization in the automobile industry is commonly observed at the research level. In the design of helmets, the use of these tools is not yet explored much by the researchers all over the world. Hence, through this thesis we tried to explore a domain for the design of helmets.

#### 3. Design of helmets for additive manufacturing

There are very limited attempts to design the safer helmets which can be manufactured using additive manufacturing. Rapid progress in the additive manufacturing technology since the past decade has made it clear that additive manufacturing will play a vital role and have a considerable share in the total production in the near future. In this work we have demonstrated some aspects regarding the design of helmets for additive manufacturing.

#### 4. Simple test procedure for helmet liners

Currently, helmets are tested using standard tests specified by some institutions. Previously only foams were used in helmets. Standard compression tests are available for testing of foams. However, when some alternatives to the foam are to be used, no simple test is present to examine the performance of the

designed structure. The only option is to test the full helmet. However full helmet tests are very time consuming and expensive to do. This thesis states a test procedure for testing energy absorbing materials especially helmet liners. The test procedure explained here is not as sophisticated as the standard full helmet tests. However, it is very simple, easy to repeat and less time consuming.

#### **4.4 Future Work**

##### **1. Standard tests using Anthropomorphic Test Devices (ATDs)**

Results of the simple benchmark example encourage us to further manufacture a prototype of helmets using the proposed ALC and test them using Anthropomorphic Test Devices(ATDs). Standard impact tests like fall test or side impact test should be performed. The guidelines for conducting these tests are provided by some institutes like Snell foundation or National Highway Traffic Safety Administration (NHTSA) Through these tests more sophisticated parameters like Head Injury Criteria (HIC), Severity Index (SI), linear and angular rotation at the neck can be obtained.

##### **2. Design of ALC for other applications**

As explained earlier the design procedure for ALC is a parametric procedure and many variants can be produced depending on the requirements for the particular application. For use in vehicle crashworthy components, the all the materials used here like ABS, PC and TangoBlack can be replaced by grades of steels and aluminum. Currently automobile bodies have a combination of ultra-high strength steels, low carbon steels, aluminum, etc. These metals can be used in the design of ALC for the use in automobile components. The parameters like volume fraction of each material needs to be decided separately each time for the new design. Similar steps can be followed for the design of ALC for use in applications like protective gears, suspension systems, combat equipments, etc.

### **3. Tests other than the impact test**

The temperature of the helmet liner sometimes may raise to a range of 115-120 °C. It is very important to cool down the helmet quickly during the operation. Hence, we suggest that the thermal analysis of helmet should be carried out in future. Besides that performance of ALC should be assessed for blast wave mitigation and noise, vibration and harshness (NVH).

### **4. Alternative manufacturing process and commercialization**

The additive manufacturing is perceived as a useful rapid prototyping process. Use of additive manufacturing for commercial batch production is practically not possible and affordable at present. In future, there are hopes that additive manufacturing will overcome this hurdle. But for near future it will be beneficial to find alternative affordable manufacturing methods for ALC.

## LIST OF REFERENCES

## LIST OF REFERENCES

- [1] G. S. Solomon, K. M. Johnston, and M. R. Lovell, *The heads-up on sport concussion*. Human Kinetics, 2006.
- [2] A. L. Petraglia, J. E. Bailes, and A. L. Day, *Handbook of Neurological Sports medicine*. Champaign, USA: Human Kinetics, 2015.
- [3] P. D. Bois, C. C. Clifford, B. B. Fileta, T. B. K. A. I. King, and J. W. H F Mahmood, J H Mertz, *Vehicle crashworthiness and occupant protection*. USA: American Iron and Steel Institute (AISI), 2004.
- [4] T.-L. Teng, C.-L. Liang, and V.-H. Nguyen, “Development and validation of finite element model of helmet impact test,” *Proceedings of the Institution of Mechanical Engineers, Part L: Journal of Materials Design and Applications*, vol. 227, no. 1, pp. 82–88, 2013.
- [5] D. C. Viano, C. Withnall, and D. Halstead, “Impact performance of modern football helmets,” *Annals of biomedical engineering*, vol. 40, no. 1, pp. 160–174, 2012.
- [6] N. J. Mills, S. Wilkes, S. Derler, and A. Flisch, “Fea of oblique impact tests on a motorcycle helmet,” *International Journal of Impact Engineering*, vol. 36, no. 7, pp. 913–925, 2009.
- [7] M. E. Carey, M. Herz, B. Corner, J. McEntire, D. Malabarba, S. Paquette, and J. B. Sampson, “Ballistic helmets and aspects of their design,” *Neurosurgery*, vol. 47, no. 3, pp. 678–689, 2000.
- [8] D. C. Viano and D. Halstead, “Change in size and impact performance of football helmets from the 1970s to 2010,” *Annals of biomedical engineering*, vol. 40, no. 1, pp. 175–184, 2012.
- [9] H.-W. Henn, “Crash tests and the head injury criterion,” *Teaching mathematics and its applications*, vol. 17, no. 4, pp. 162–170, 1998.
- [10] P. Honarmandi, A. M. Sadegh, and P. V. Cavallaro, “Do american football helmets protect players against concussions?,” in *ASME 2013 International Mechanical Engineering Congress and Exposition*, pp. V03BT03A052–V03BT03A052, American Society of Mechanical Engineers, 2013.
- [11] A. Karimi, M. Navidbakhsh, and R. Razaghi, “An experimental-finite element analysis on the kinetic energy absorption capacity of polyvinyl alcohol sponge,” *Materials Science and Engineering: C*, vol. 39, pp. 253–258, 2014.
- [12] G. D. Caserta, L. Iannucci, and U. Galvanetto, “Shock absorption performance of a motorbike helmet with honeycomb reinforced liner,” *Composite Structures*, vol. 93, no. 11, pp. 2748–2759, 2011.

- [13] M. F. Rueda, L. Cui, and M. Gilchrist, "Optimisation of energy absorbing liner for equestrian helmets. part i: Layered foam liner," *Materials & Design*, vol. 30, no. 9, pp. 3405–3413, 2009.
- [14] L. Cui, M. F. Rueda, and M. Gilchrist, "Optimisation of energy absorbing liner for equestrian helmets. part ii: Functionally graded foam liner," *Materials & Design*, vol. 30, no. 9, pp. 3414–3419, 2009.
- [15] F. Shuaeib, A. Hamouda, S. Wong, R. R. Umar, and M. M. Ahmed, "A new motorcycle helmet liner material: The finite element simulation and design of experiment optimization," *Materials & design*, vol. 28, no. 1, pp. 182–195, 2007.
- [16] N. Gupta and V. C. Shunmugasamy, "High strain rate compressive response of syntactic foams: Trends in mechanical properties and failure mechanisms," *Materials Science and Engineering: A*, vol. 528, no. 25, pp. 7596–7605, 2011.
- [17] V. V. Gokhale, C. Marko, T. Alam, P. Chaudhari, and A. Tovar, "Design of an advanced layered composite for energy dissipation using a 3d-lattice of micro compliant mechanism," tech. rep., SAE Technical Paper, 2016.
- [18] S. S. Tolman, "Elastic energy absorption via compliant corrugations," 2014.
- [19] J. E. Hyland, M. I. Frecker, and G. A. Lesieutre, "Optimization of honeycomb contact-aided compliant cellular mechanism for strain energy absorption," in *ASME 2012 International Design Engineering Technical Conferences and Computers and Information in Engineering Conference*, pp. 311–320, American Society of Mechanical Engineers, 2012.
- [20] C. A. Nelson, "A compliant straight-line shock absorption mechanism using a viscoelastic pseudo-rigid body model," in *ASME 2009 International Design Engineering Technical Conferences and Computers and Information in Engineering Conference*, pp. 233–240, American Society of Mechanical Engineers, 2009.
- [21] A. E. Albanesi, V. D. Fachinotti, and M. A. Pucheta, "A review on design methods for compliant mechanisms," *Mecánica Computacional*, vol. 29, no. 3, 2010.
- [22] L. L. Howell and A. Midha, "Parametric deflection approximations for end-loaded, large-deflection beams in compliant mechanisms," *Journal of Mechanical Design*, vol. 117, no. 1, pp. 156–165, 1995.
- [23] L. L. Howell, A. Midha, and T. Norton, "Evaluation of equivalent spring stiffness for use in a pseudo-rigid-body model of large-deflection compliant mechanisms," *Journal of Mechanical Design*, vol. 118, no. 1, pp. 126–131, 1996.
- [24] J. Pauly and A. Midha, "Improved pseudo-rigid-body model parameter values for end-force-loaded compliant beams," in *ASME 2004 International Design Engineering Technical Conferences and Computers and Information in Engineering Conference*, pp. 1513–1517, American Society of Mechanical Engineers, 2004.
- [25] S. Jagirdar and C. P. Lusk, "Preliminaries for a spherical compliant mechanism: pseudo-rigid-body model kinematics," in *ASME 2007 International Design Engineering Technical Conferences and Computers and Information in Engineering Conference*, pp. 55–66, American Society of Mechanical Engineers, 2007.

- [26] X. Pei, J. Yu, G. Zong, and S. Bi, “An effective pseudo-rigid-body method for beam-based compliant mechanisms,” *Precision Engineering*, vol. 34, no. 3, pp. 634–639, 2010.
- [27] L. C. Leishman and M. B. Colton, “A pseudo-rigid-body model approach for the design of compliant mechanism springs for prescribed force-deflections,” in *ASME 2011 International Design Engineering Technical Conferences and Computers and Information in Engineering Conference*, pp. 93–102, American Society of Mechanical Engineers, 2011.
- [28] A. E. Albanesi, V. D. Fachinotti, and A. Cardona, “Inverse finite element method for large-displacement beams,” *International Journal for Numerical Methods in Engineering*, vol. 84, no. 10, pp. 1166–1182, 2010.
- [29] V. D. Fachinotti, A. Cardona, and P. Jetteur, “Finite element modelling of inverse design problems in large deformations anisotropic hyperelasticity,” *International Journal for Numerical Methods in Engineering*, vol. 74, no. 6, pp. 894–910, 2008.
- [30] X. Huang, Y. Xie, and G. Lu, “Topology optimization of energy-absorbing structures,” *International Journal of Crashworthiness*, vol. 12, no. 6, pp. 663–675, 2007.
- [31] B. Q. Wang, B. L. Wang, and Z. Y. Huang, “Topology optimization for constrained layer damping plates using evolutionary structural optimization method,” in *Advanced Materials Research*, vol. 894, pp. 158–162, Trans Tech Publ, 2014.
- [32] D. Stojanov, B. G. Falzon, X. Wu, and W. Yan, “An application of bi-directional evolutionary structural optimisation for optimising energy absorbing structures using a material damage model,” *Applied Mechanics & Materials*, no. 553, 2014.
- [33] X. Huang and Y. Xie, “Topology optimization of nonlinear structures under displacement loading,” *Engineering structures*, vol. 30, no. 7, pp. 2057–2068, 2008.
- [34] R. A. Wildman and G. A. Gazonas, “Multiobjective topology optimization of energy absorbing materials,” *Structural and Multidisciplinary Optimization*, vol. 51, no. 1, pp. 125–143, 2015.
- [35] D. Jung and H. C. Gea, “Design of energy absorbing structure using topology optimization with a multi-material model,” in *ASME 2003 International Design Engineering Technical Conferences and Computers and Information in Engineering Conference*, pp. 683–691, American Society of Mechanical Engineers, 2003.
- [36] N. M. Patel, B.-S. Kang, and J. E. Renaud, “Crashworthiness design using a hybrid cellular automaton algorithm,” in *ASME 2006 International Design Engineering Technical Conferences and Computers and Information in Engineering Conference*, pp. 151–162, American Society of Mechanical Engineers, 2006.
- [37] P. Bandi, J. P. Schmiedeler, and A. Tovar, “Design of crashworthy structures with controlled energy absorption in the hybrid cellular automaton framework,” *Journal of Mechanical Design*, vol. 135, no. 9, p. 091002, 2013.

- [38] L. Guo, A. Tovar, C. L. Penninger, and J. E. Renaud, “Strain-based topology optimisation for crashworthiness using hybrid cellular automata,” *International Journal of Crashworthiness*, vol. 16, no. 3, pp. 239–252, 2011.
- [39] L. S. Guo, J. Huang, A. Tavor, and J. E. Renaud, “Multidomain topology optimization for crashworthiness based on hybrid cellular automata,” in *Key Engineering Materials*, vol. 486, pp. 250–253, Trans Tech Publ, 2011.
- [40] G. K. Ananthasuresh, *A new design paradigm for micro-electro-mechanical systems & investigations on the compliant mechanism synthesis*. University of Michigan, 1994.
- [41] O. Sigmund, “On the design of compliant mechanisms using topology optimization\*,” *Journal of Structural Mechanics*, vol. 25, no. 4, pp. 493–524, 1997.
- [42] S. Nishiwaki, M. I. Frecker, S. Min, and N. Kikuchi, “Topology optimization of compliant mechanisms using the homogenization method,” *International Journal for Numerical Methods in Engineering*, vol. 42, no. 3, pp. 535–559, 1998.
- [43] T. E. Bruns and D. A. Tortorelli, “Topology optimization of non-linear elastic structures and compliant mechanisms,” *Computer Methods in Applied Mechanics and Engineering*, vol. 190, no. 26, pp. 3443–3459, 2001.
- [44] D. Jung and H. C. Gea, “Compliant mechanism design with non-linear materials using topology optimization,” in *ASME 2002 International Design Engineering Technical Conferences and Computers and Information in Engineering Conference*, pp. 1079–1087, American Society of Mechanical Engineers, 2002.
- [45] X. Huang, Y. Li, S. Zhou, and Y. Xie, “Topology optimization of compliant mechanisms with desired structural stiffness,” *Engineering Structures*, vol. 79, pp. 13–21, 2014.
- [46] A. Saxena, “Topology design of large displacement compliant mechanisms with multiple materials and multiple output ports,” *Structural and Multidisciplinary Optimization*, vol. 30, no. 6, pp. 477–490, 2005.
- [47] K. Liu and A. Tovar, “An efficient 3d topology optimization code written in matlab,” *Structural and Multidisciplinary Optimization*, vol. 50, no. 6, pp. 1175–1196, 2014.
- [48] E. Andreassen, A. Clausen, M. Schevenels, B. S. Lazarov, and O. Sigmund, “Efficient topology optimization in matlab using 88 lines of code,” *Structural and Multidisciplinary Optimization*, vol. 43, no. 1, pp. 1–16, 2011.
- [49] M. P. Bendsøe, “Optimal shape design as a material distribution problem,” *Structural optimization*, vol. 1, no. 4, pp. 193–202, 1989.
- [50] N. Meisel, A. Gaynor, C. Williams, and J. Guest, “Multiple-material topology optimization of compliant mechanisms created via polyjet 3d printing,” in *24th Annual International Solid Freeform Fabrication Symposium—An Additive Manufacturing Conference*, 2013.
- [51] R. Tavakoli and S. M. Mohseni, “Alternating active-phase algorithm for multi-material topology optimization problems: a 115-line matlab implementation,” *Structural and Multidisciplinary Optimization*, vol. 49, no. 4, pp. 621–642, 2014.



- [52] I. Gibson, D. Rosen, and B. Stucker, *Additive manufacturing technologies*. Springer, 2010.
- [53] E. Klompen, T. Engels, L. Van Breemen, P. Schreurs, L. Govaert, and H. Meijer, “Quantitative prediction of long-term failure of polycarbonate,” *Macromolecules*, vol. 38, no. 16, pp. 7009–7017, 2005.